SEMI-FINAL REPORT No. 4

under

Grant No. N00014-90-J-1526

on

DETAILED ANALYSIS OF THE STORM SURGE CAUSED BY TYPHOON NANCY OF 1961 IN WEST CENTRAL JAPAN

by

T. Theodore Fujita

to

Department of the Navy
Office of Naval Research
800 Quincy Street
Arlington, VA 22217

monitored by

Dr. Robert F. Abbey, Jr.
Marine Meteorology Program
Office of Naval Research

PREFACE

Although Typhoon Nancy of 1961 occurred some 34 years ago in western Japan, the air-sea interaction data obtained by Japan Meteorological Agency during the storm were excellent.

Radar data from the Murato station atop the 810 ft. cliff overlooking the Pacific Ocean are by no means comparable to those from modernized Doppler radars. Nevertheless, their imagery is good enough to assess the typhoon-induced rain areas and their movement.

Coverage of tide gages, both in area and density is excellent. The data permit the author to determine accurately the storm-surge patterns at 10- to 60-minute intervals.

The analytical results revealed, for the first time, the progress of typhoon-induced high tides affected by the pressure field, wind stress, and topographic influences.

The author attempted to obtain high-resolution data of the storm surge induced by hurricane Andrew of 24 August 1992 in south Florida and Hurricane Iniki of 11 September 1992 in Kauai, Hawaii. Unfortunately, no such data comparable to the Nancy data obtained 34 years ago in Japan was available. So-called modernized data are often inferior in resolution and data density in particular, making it very difficult to determine the time-dependent features of the storm surge.

TABLE OF CONTENTS

1. INTRODUCTION

Although it is natural to assume that the storm surge by typhoon is caused by the combined effects of (1) low pressure field and (2) high wind stress occurring simultaneously during the storm, the effects vary significantly according to the shape of the coastlines.

When a typhoon moves over complicated coastal areas, surface water must travel some distance, being pushed by the wind and elevated by the reduced pressure. In accomplishing the surge of surface water, it is necessary to evaluate the trajectories of water converging from various directions, passing through small channels or moving around islands and peninsulae. Complicated trajectories of surging water rarely occur along the U.S. coastlines in hurricane areas.

As an exchange document between the Japan Meteorological Agency (JMA) and Fujita's Wind Research Laboratory (WRL), Fujita received the Report of Muroto Typhoon II, Typhoon Nancy of September 1961. The report includes numerous data on storm surge and high winds tabulated for a period of 12 hours at 10-minute intervals. During this period, Nancy crossed central Japan from southwest to northeast inducing a 149 mph (15-min) mean wind and a 189+ mph peak gust. Although these extreme wind speeds were measured at Muroto Weather Station located atop an 810 ft. cliff, the windspeeds were very significant, leaving behing a long-term record of the historical typhoons in Japan. Presented in this report is the result of Fujita's mesoscale analysis of the rare patterns of the storm surge (anomalies).

Appreciations are due to the Japan Meteorological Agency and Fujita's colleages in Japan since the 1950's when he worked on his detailed analysis of typhoons. Fujita's ScD Thesis was Analytical Studies of Typhoons (Doctorate received in August 1953 from Tokyo University, Tokyo, Japan).

MINIMUM PRESSURE AND MAXIMUM WIND

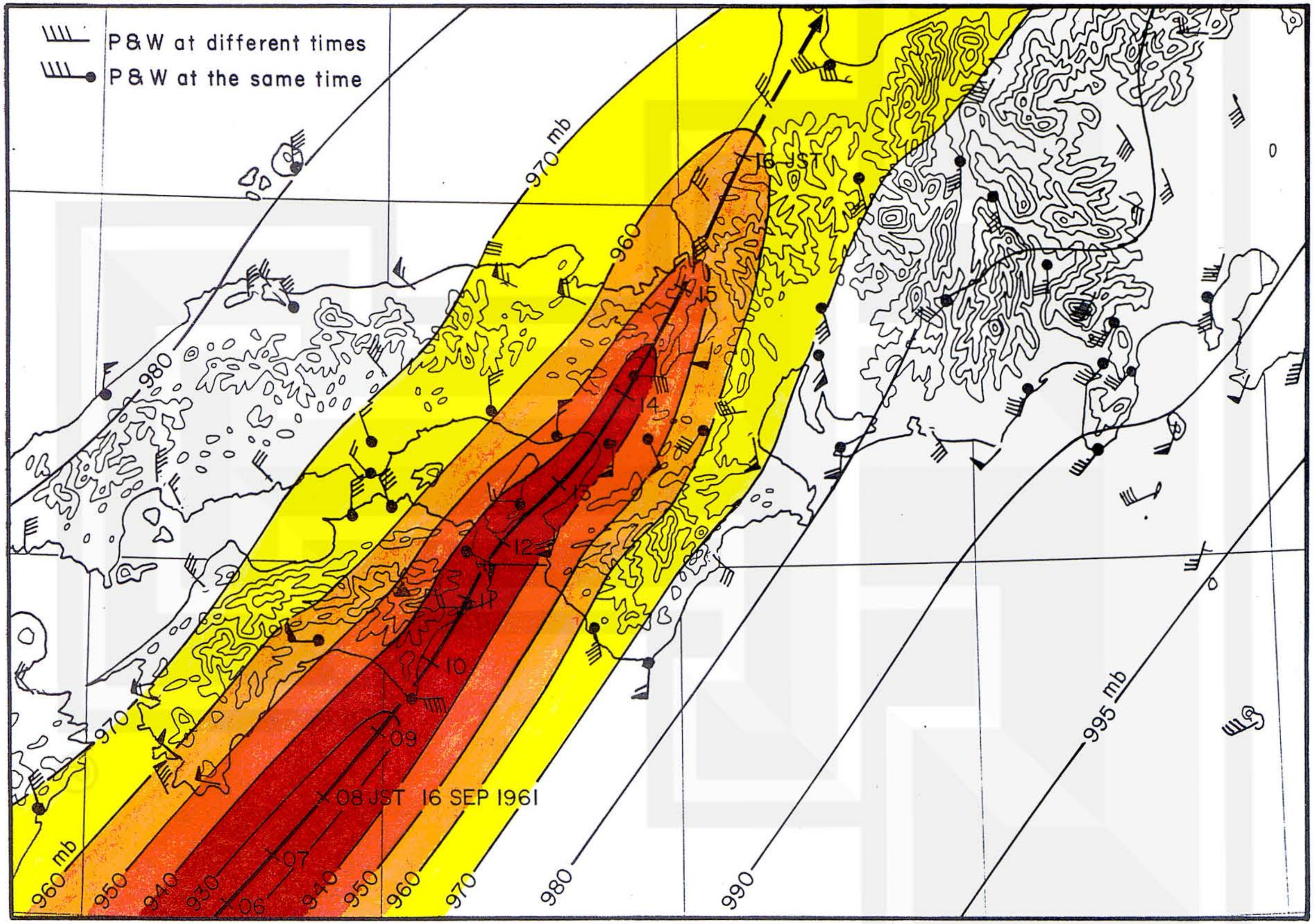

Fig. 1.1 The minimum pressure pattern of Typhoon Nancy of 1961. The 930 mb band extended to Muroto and the 940 mb, beyond Kyoto.

Contoured Minimum Pressure

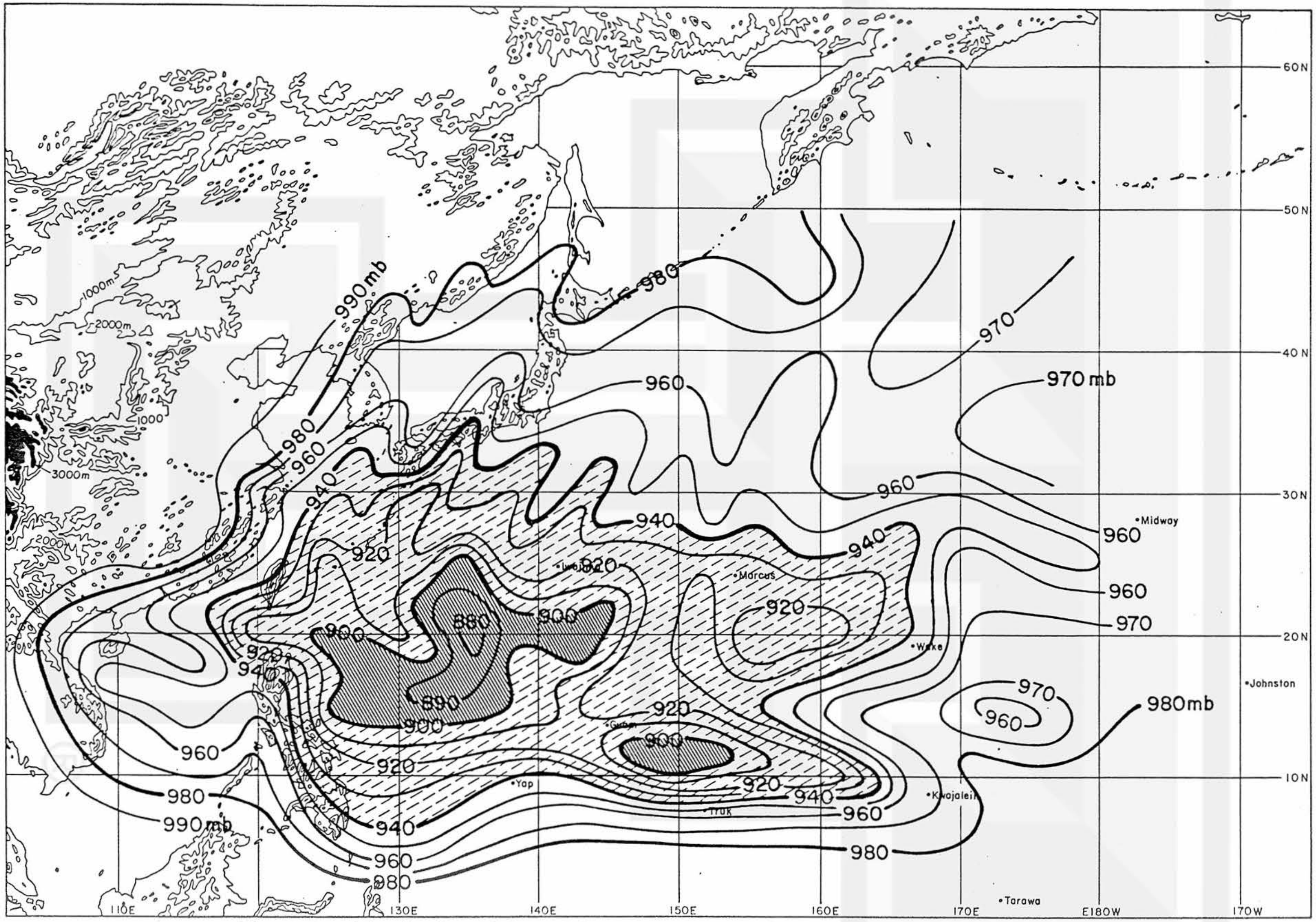

Fig. 1.2 Distribution of the minimum pressure of typhoons. Note that Typhoon Nancy which hit Osaka Bay was a very deep typhoon.

2. RADAR ECHOES FROM MUROTO STATION

The JMA Muroto radar (5cm) is located 1 km (0.6 mile) north of the southern tip of Cape Muroto (Fig. 2.1). The height of the foundation is 185 m (810 ft.) with practically no obstuctions in most directions, except between 330° and 010° azimuths where the mountains extend toward the 1995 m (6500 ft.) Tsurugi-yama far to the north.

By virtue of the elevation of the radar, overlooking the Pacific Ocean, photographic range toward the approaching typhoon was over 325 km (200 miles). The first available picture at 0339 JST (9 hours + GMT) shows a large rainband on the north to southeast sectors of the eye. The dark areas arround the radar are interference and sea clutter (Fig. 2.2). The radar echo depiction at 0545 JST shows both outer and inner bands (Fig. 2.3). The outer band in the northeast sector began disappearing into the sea clutter.

As the typhoon center began entering the open bay (called Tosa-bay) south of Shikoku, the mountains of Shikoku distorted the pattern of the eye (Fig. 2.4). We are, nevertheless, able to identify the existence of six narrow rainbands inside the east sector of the typhoon.

The center of the eye passed directly over the radar and entered the strait between Shikoku and Kinki (Fig. 2.5). At the 1004 JST picture time the center was moving northeast off the coast of Shikoku. The rainbands extending from Shikoku to Tosa-bay distorted significantly; while rainbands inside the south to east sectors were well defined.

The last picture at 1128 JST (Fig. 2.6) reveals that the rainbands inside the downslope winds from Shikoku weakened, and some disappeared. On the other hand, the rainbands in the east to northeast sectors intensified as they approached Kinki with

1000 to 1600 m (3000 to 5000 ft.) mountains. At this time the central pressure was still 935 mb.

Thereafter, the typhoon center entered Osaka Bay, causing a significant storm surge. The typhoon left behind the maximum total rainfall of 1,162 mm (93 inches) over the east Shikoku mountains, causing flash floods and landslides at numerous locations. 185 persons were killed and 3,879 others were injured.

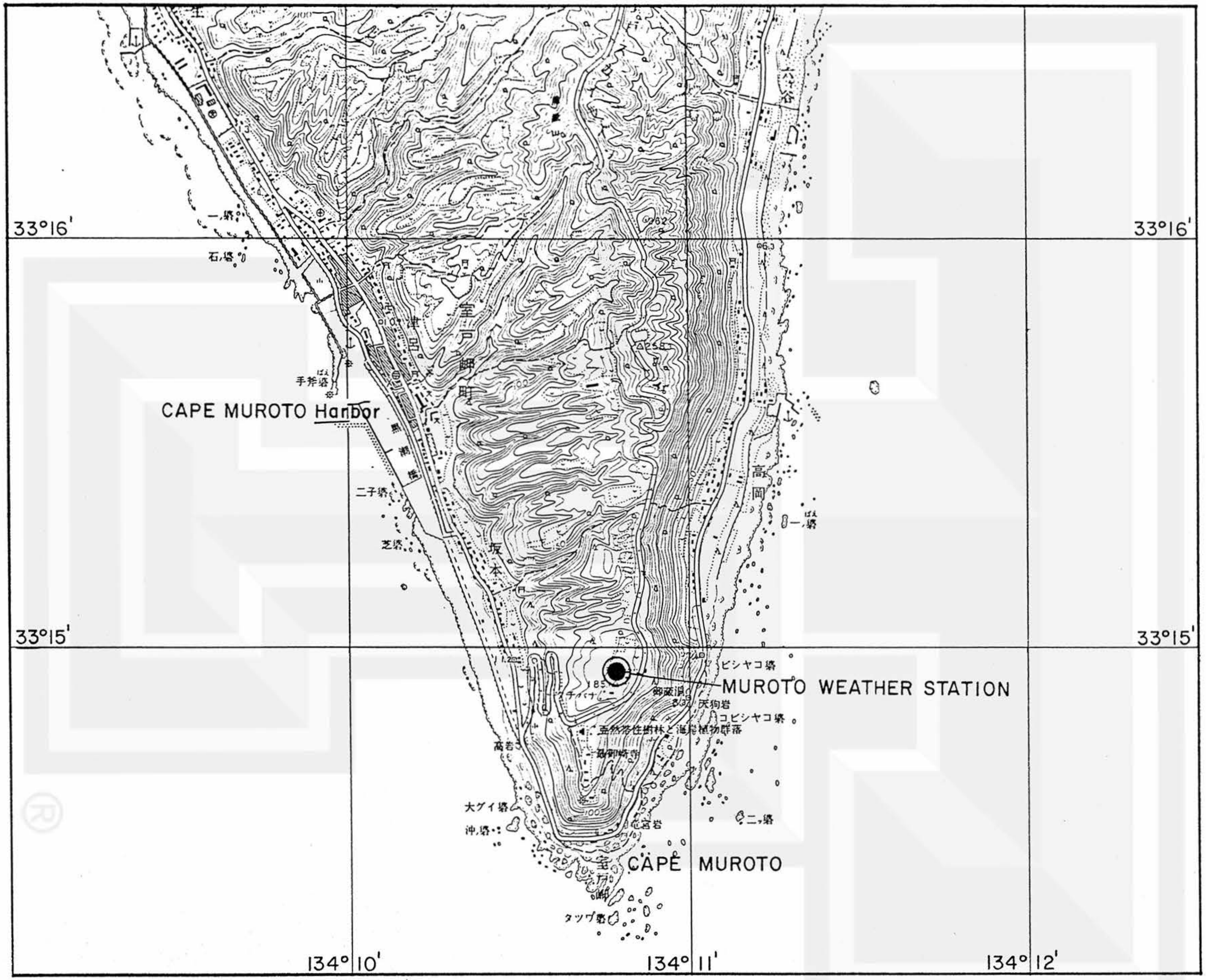

Fig. 2.1 Muroto Weather Station located atop a 185 m (810 ft) cliff. The anemometer recorded a 66.7 m/s (149 mph) 15-minute maximum wind and 84.5+ m/s (189+ mph) peak gust.

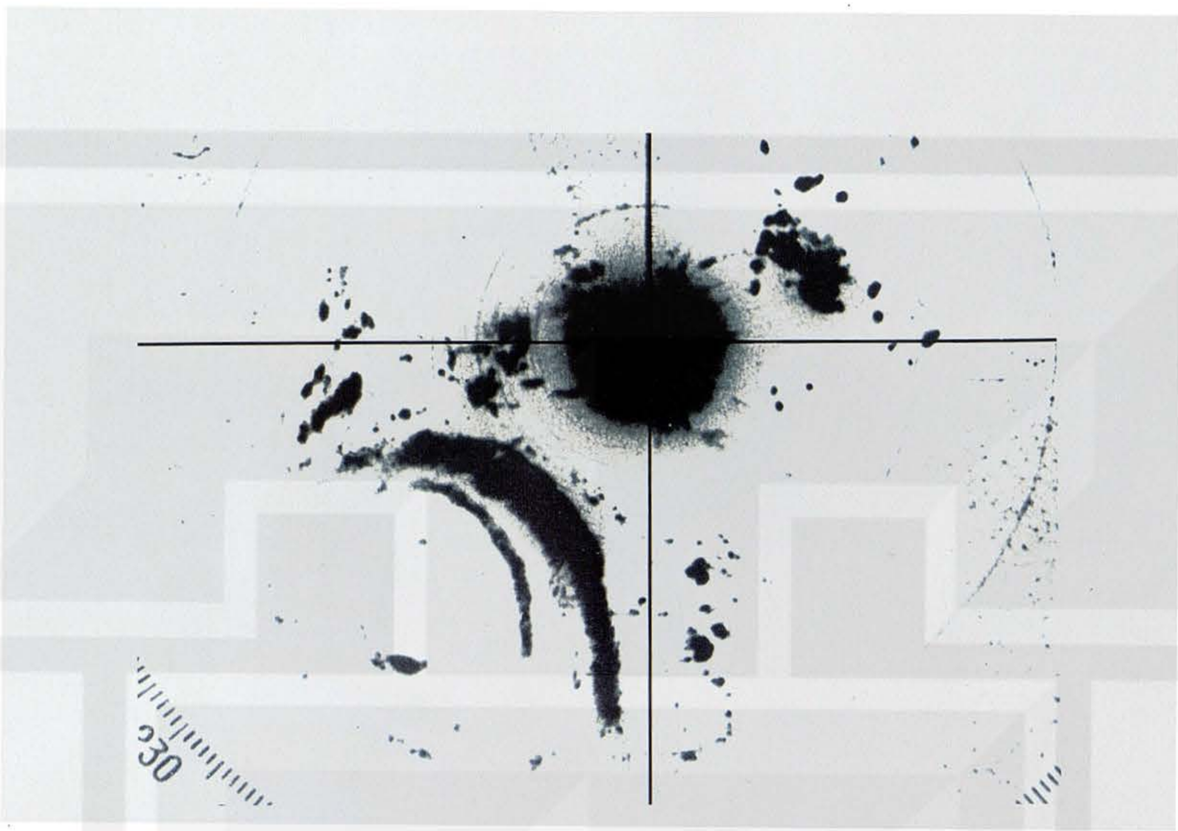

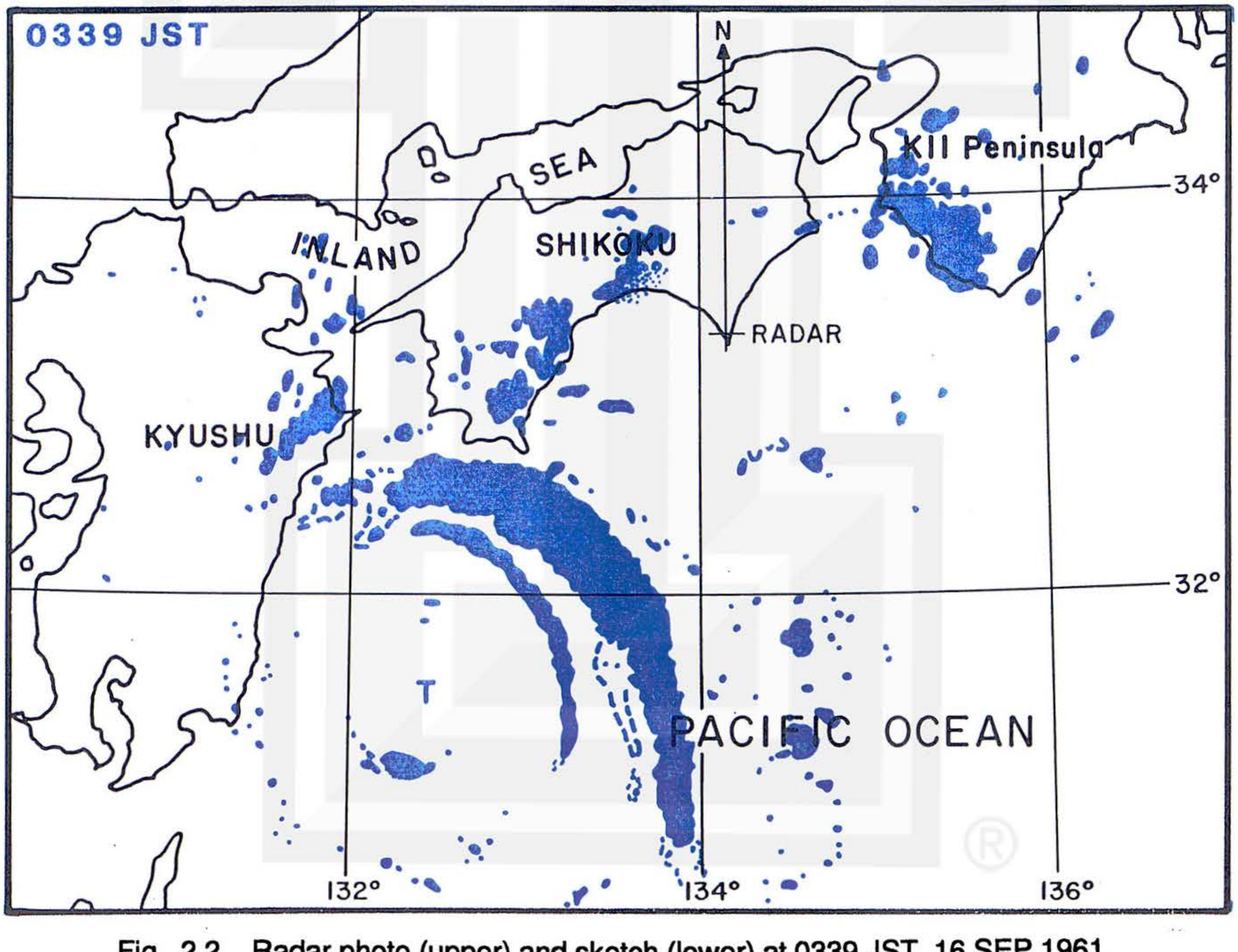

Fig. 2.2 Radar photo (upper) and sketch (lower) at 0339 JST, 16 SEP 1961.

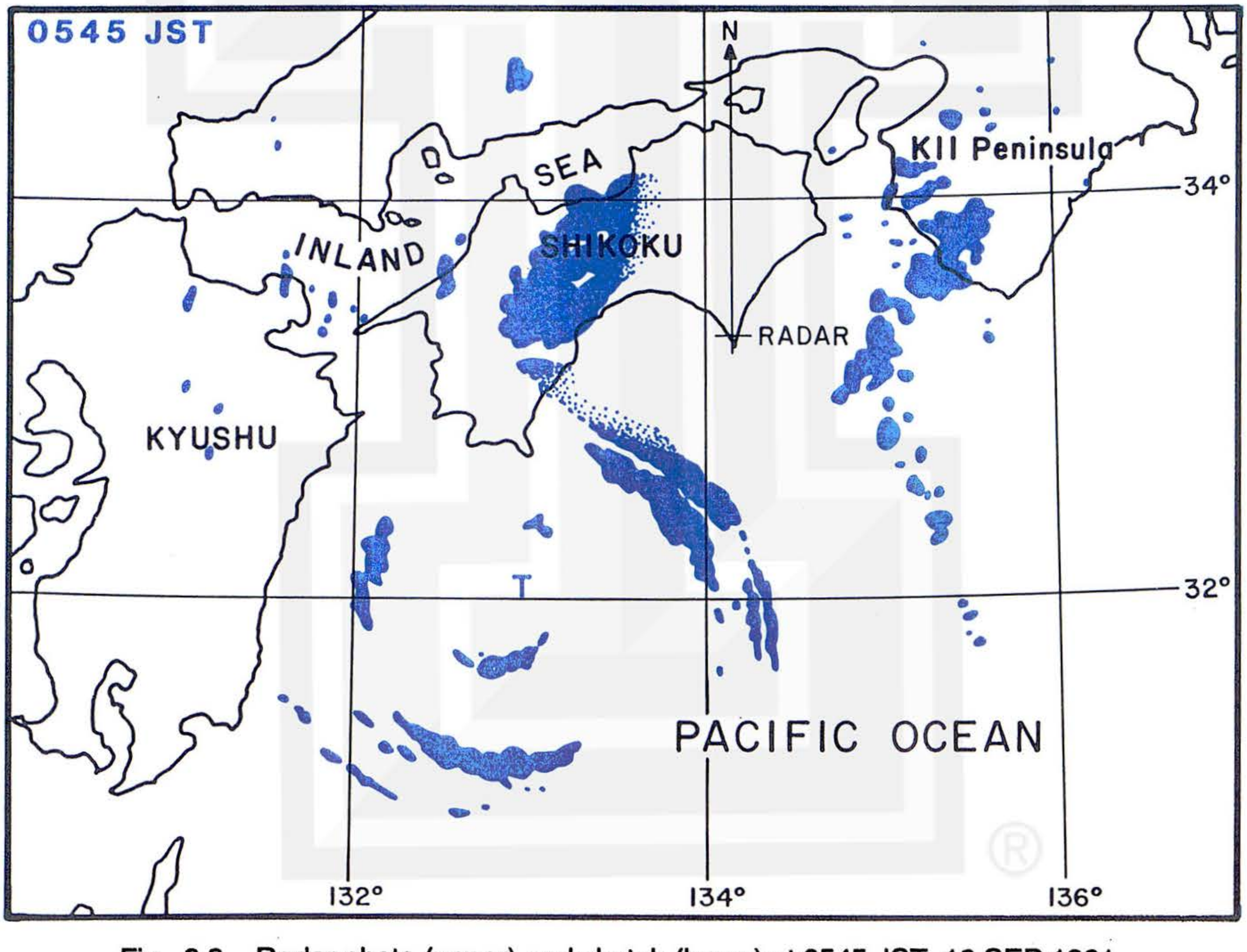

Fig. 2.3 Radar photo (upper) and sketch (lower) at 0545 JST, 16 SEP 1961.

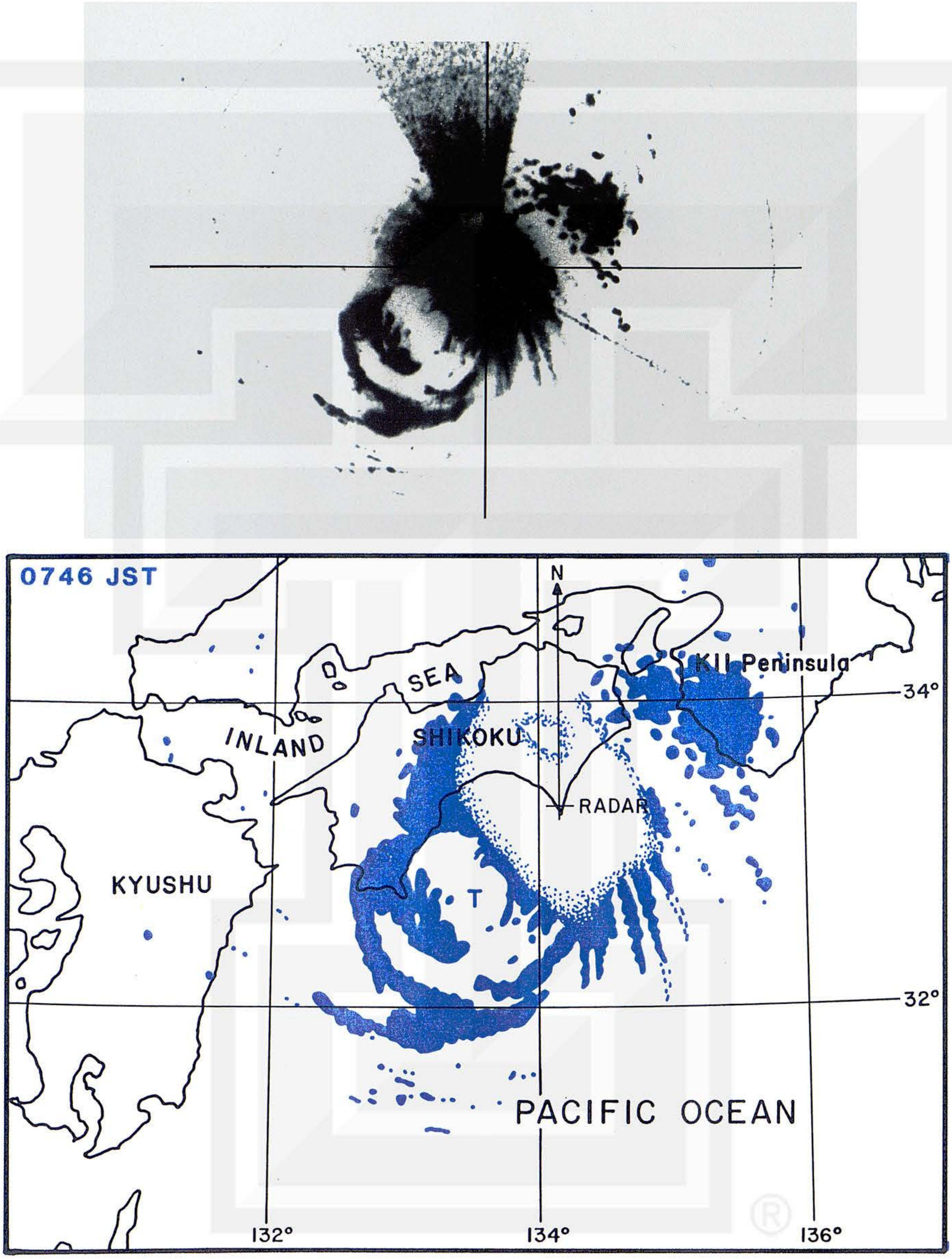

Fig. 2.4 Radar photo (upper) and sketch (lower) at 0746 JST, 16 SEP 1961.

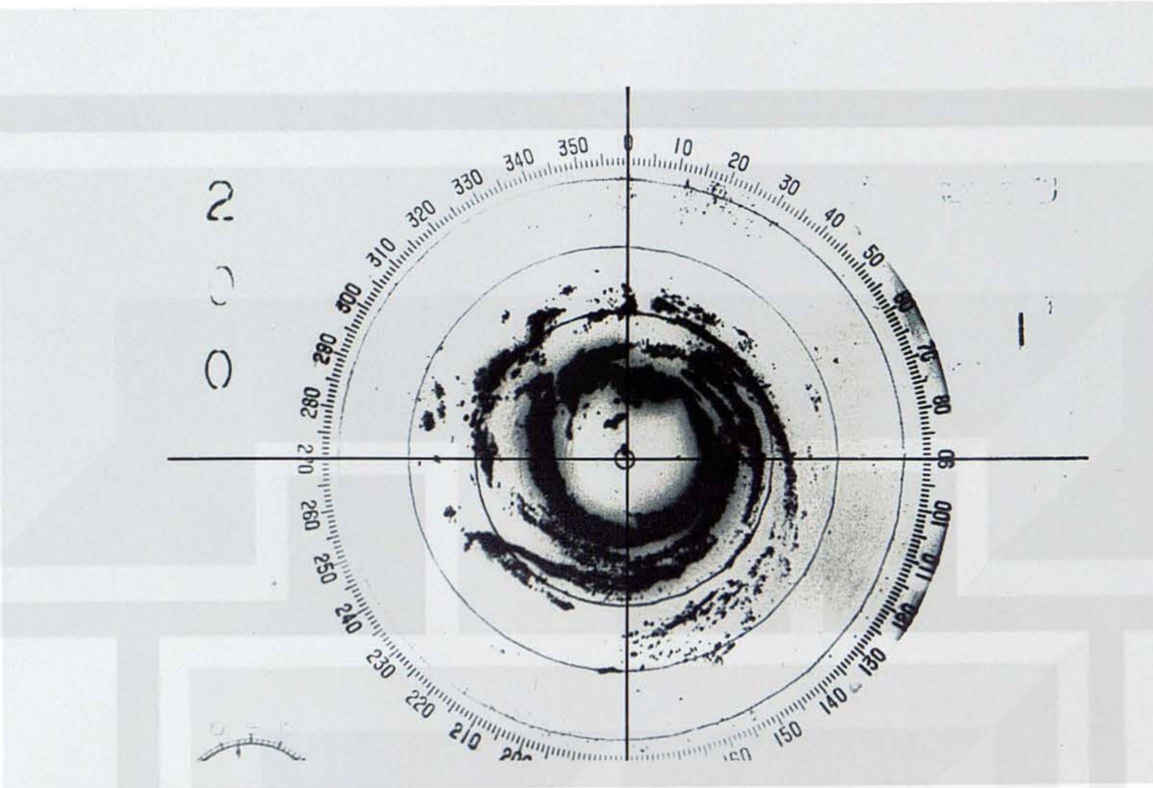

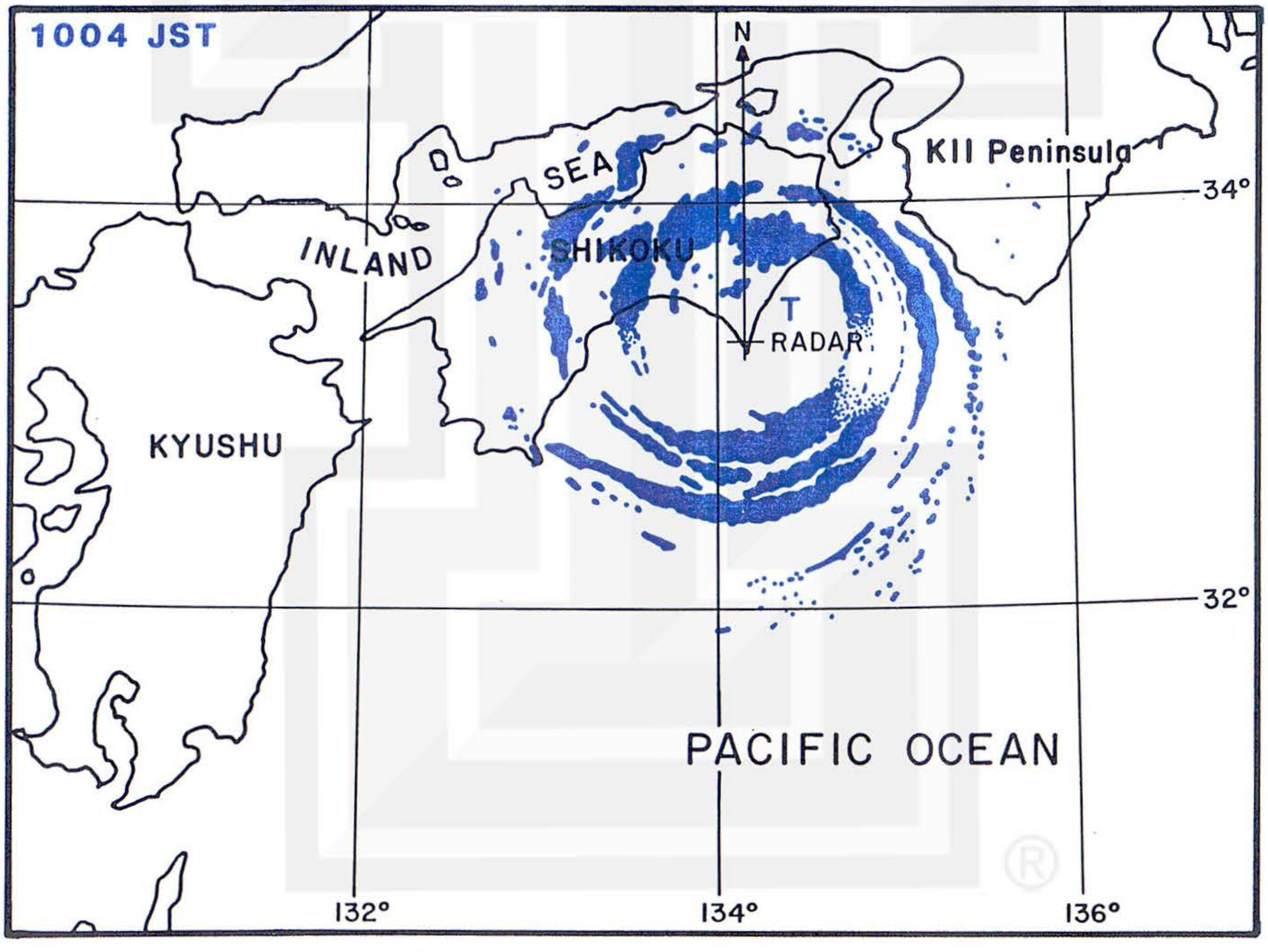

Fig. 2.5 Radar photo (upper) and sketch (lower) at 1004 JST, 16 SEP 1961.

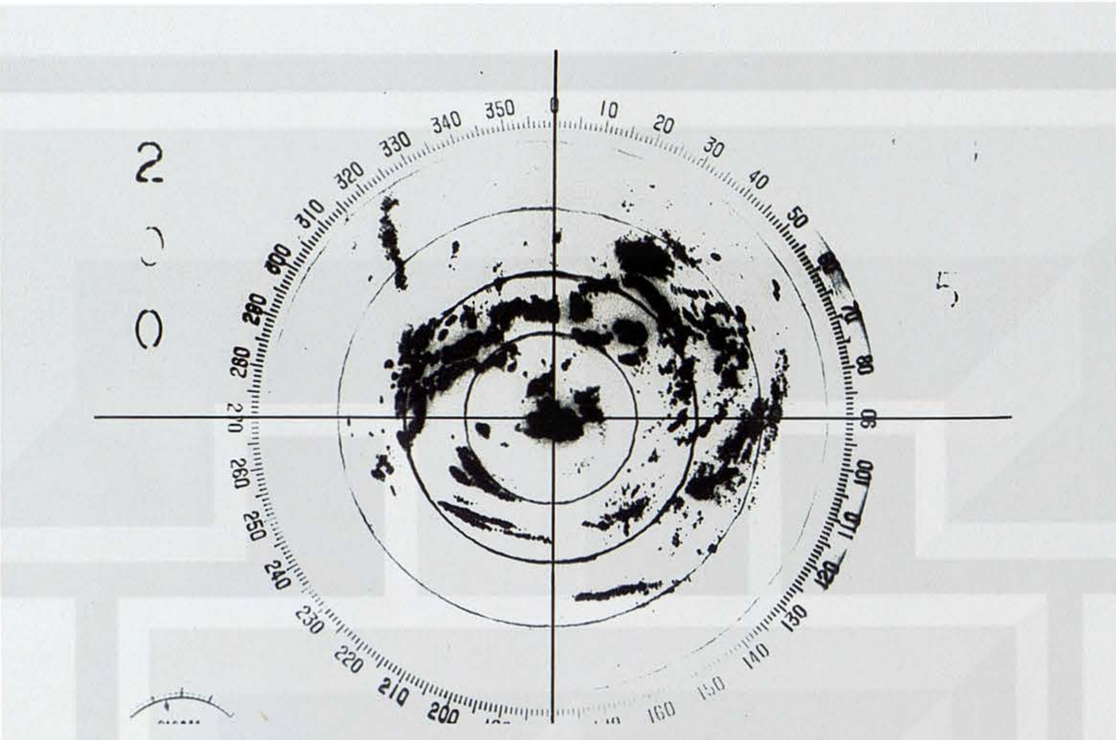

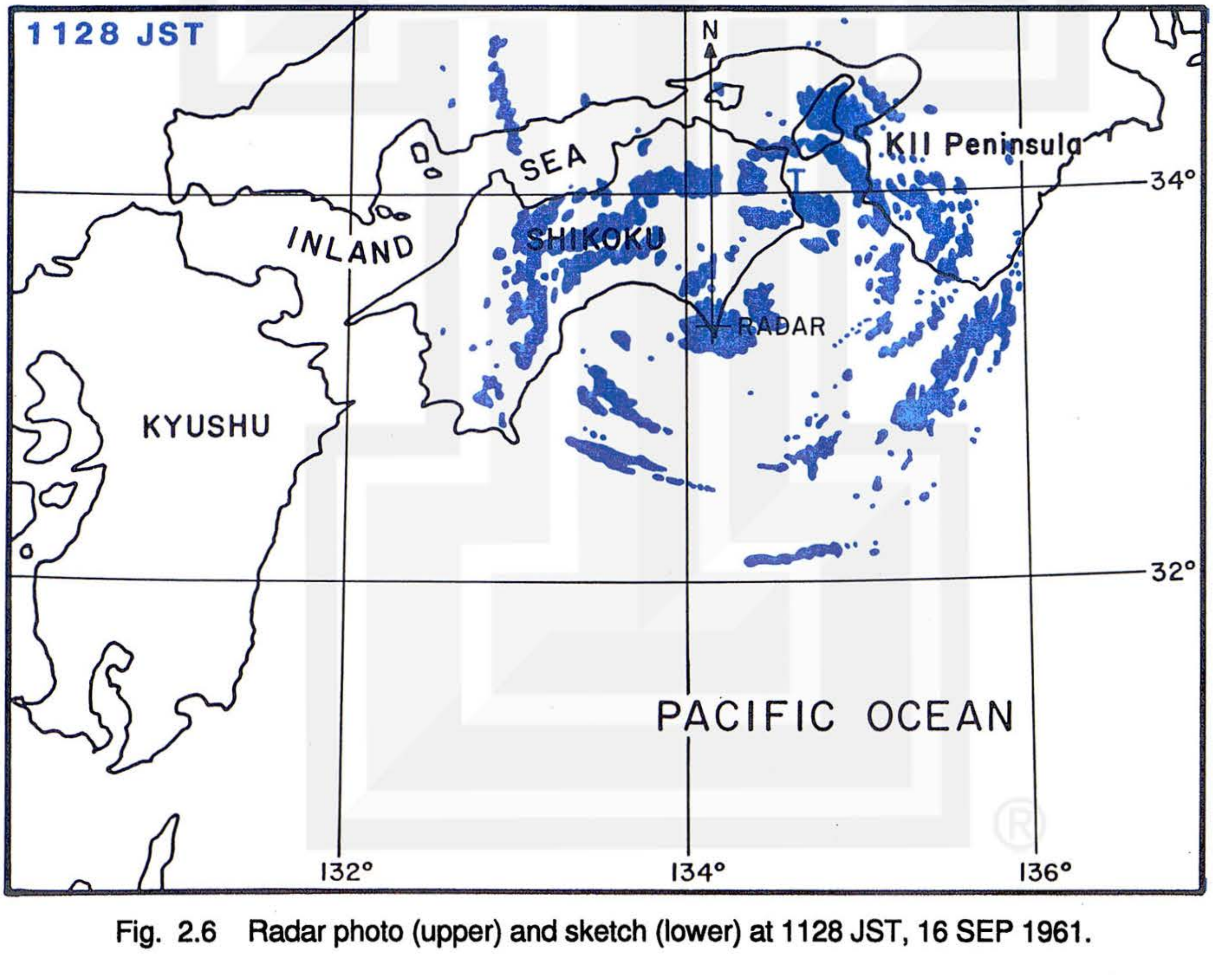

Fig. 2.6 Radar photo (upper) and sketch (lower) at 1128 JST, 16 SEP 1961.

3. DISTRIBUTION OF TIDE-GAGE STATIONS

The JMA Report of Typhoon Nancy of 1961 includes the tide-gage data from 47 stations inside the disturbance areas. Of these there are two groups:

Hourly-data stations............................1-12, 35-38, and 41-47; and

10-minute-data stations.......................13-34, and 39-40.

In other words, of 47 stations hourly data are available from 23 stations while 10-minute data, from 24 stations. These data were utilized to perform synoptic-scale analysis first, and mesoscale analysis later.

Presented in this section is the environmental map of each tide-gage station used in the storm-surge analyses. It should be mentioned, however, that exact locations of tide gages are not available from all 47 stations. Best-possible estimates were made in producing Figures 3.1 through 3.47.

Distribution of Tide-Gage Stations

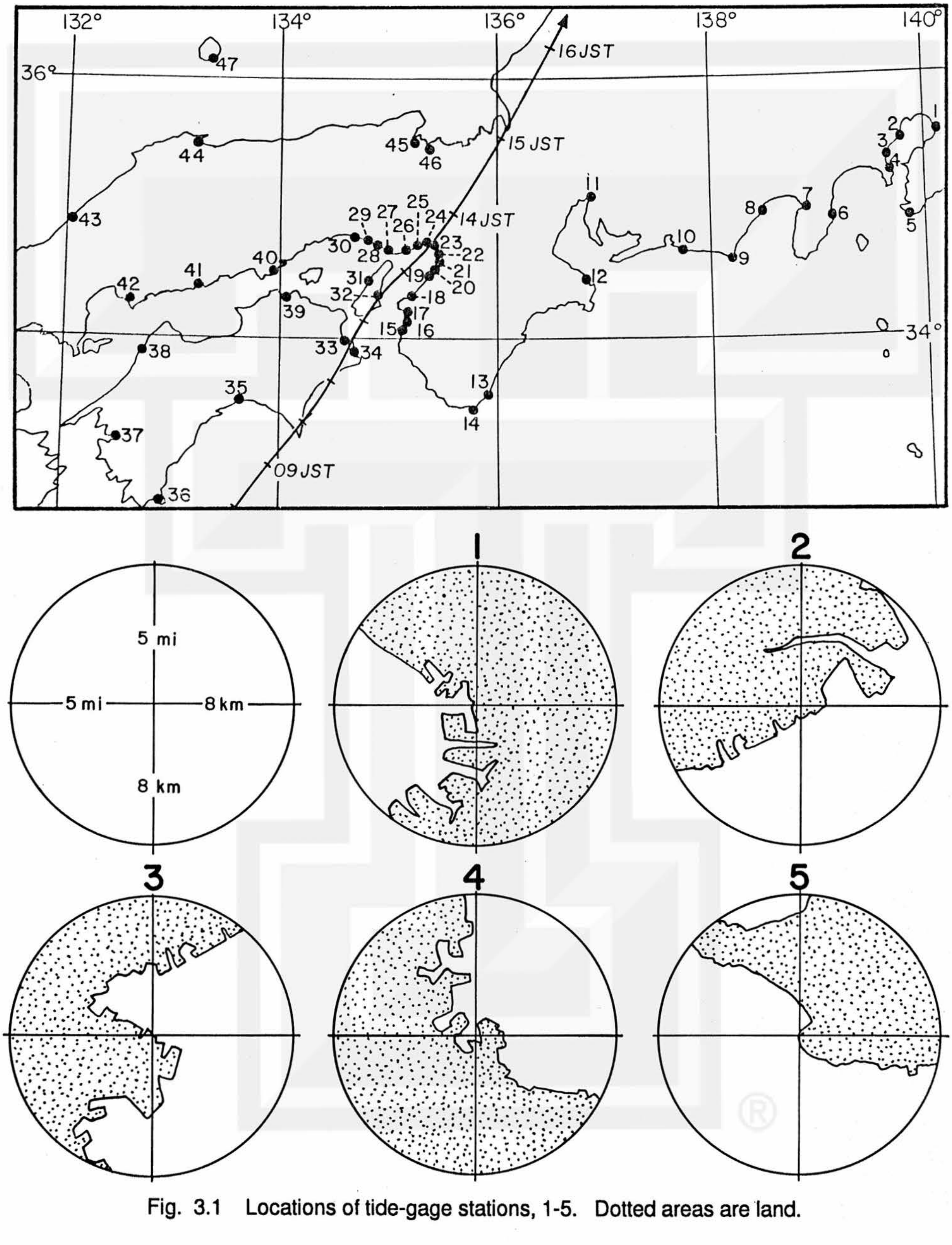

Fig. 3.1 Locations of tide-gage stations, 1-5. Dotted areas are land.

Distribution of Tide-Gage Stations

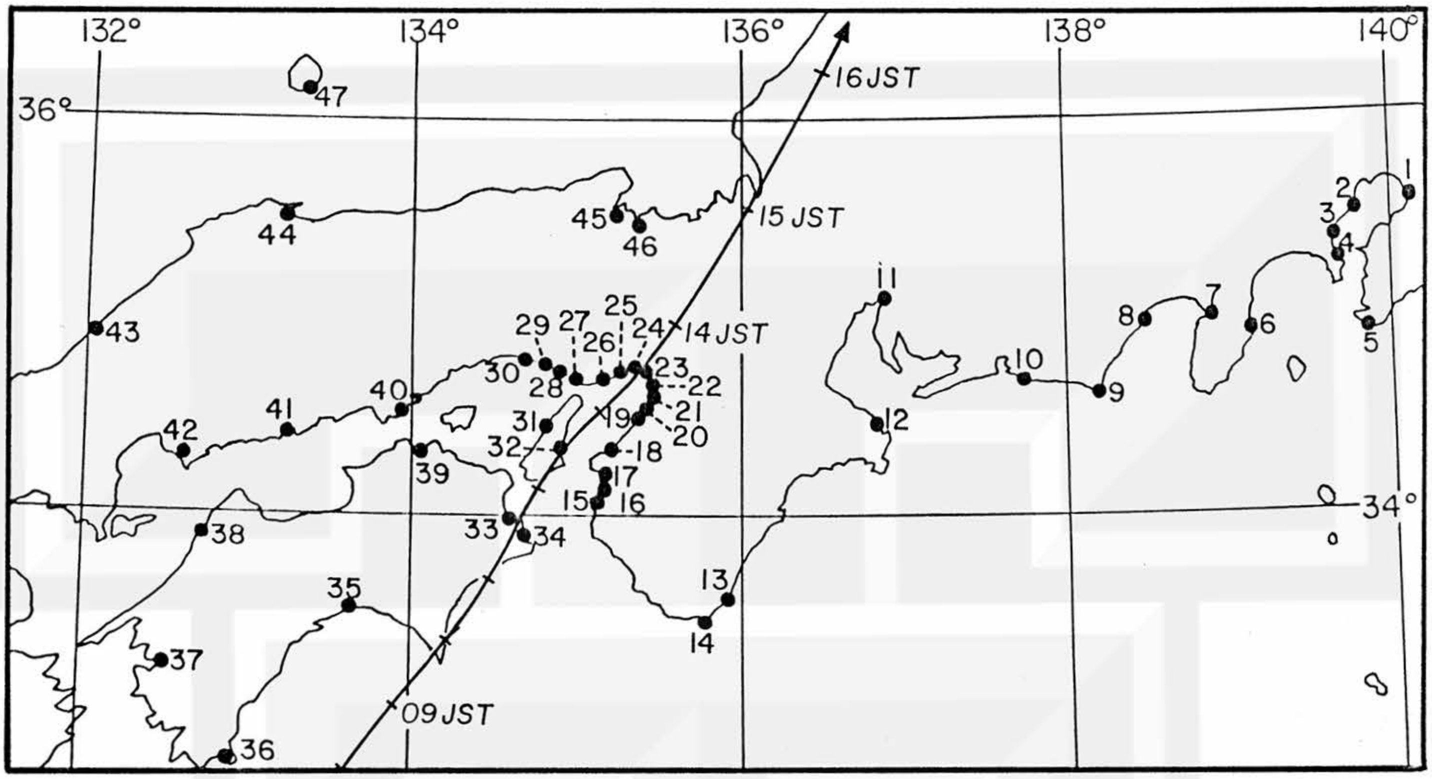

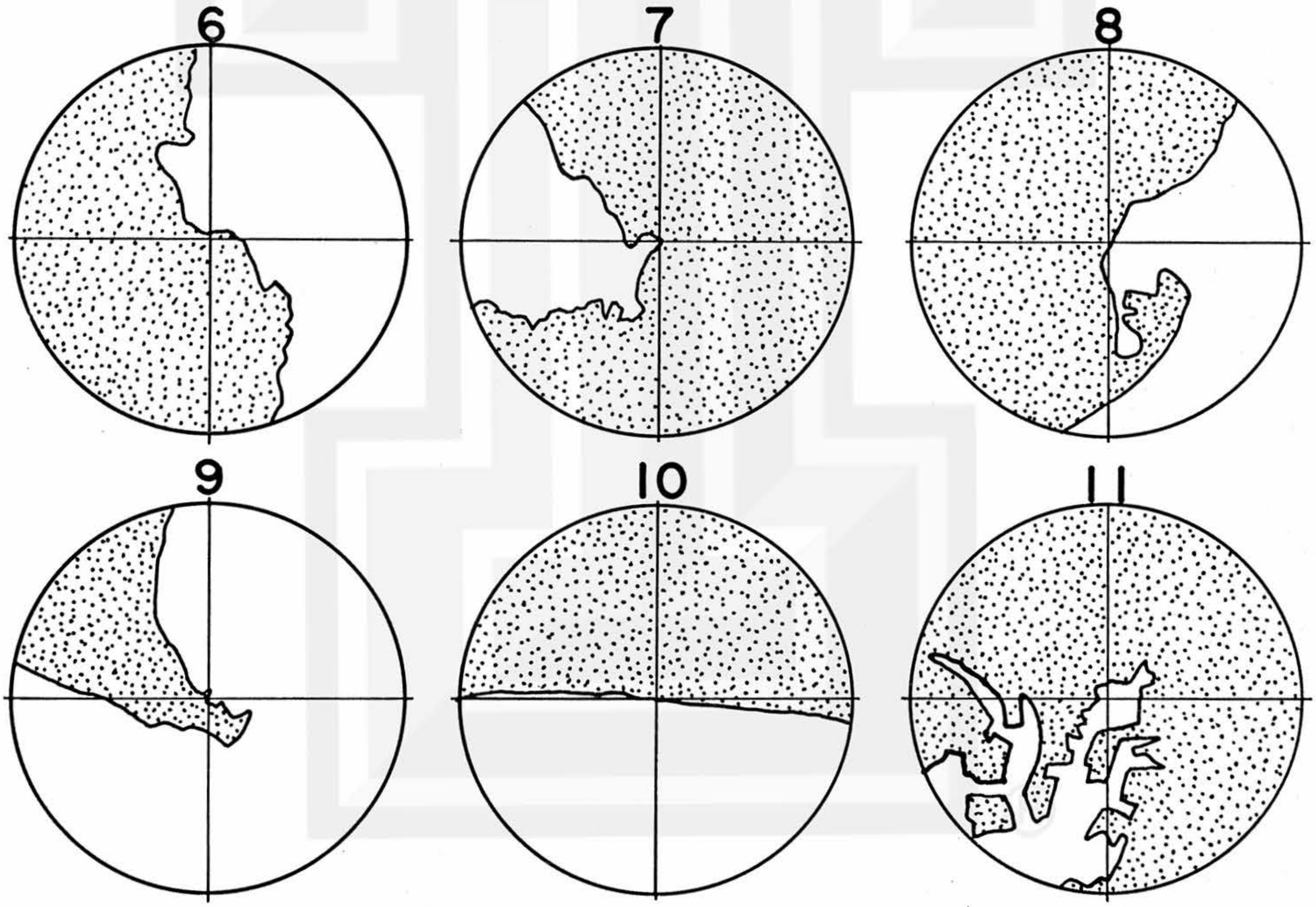

Fig. 3.2 Locations of tide-gage stations, 6-11.

Distribution of Tide-Gage Stations

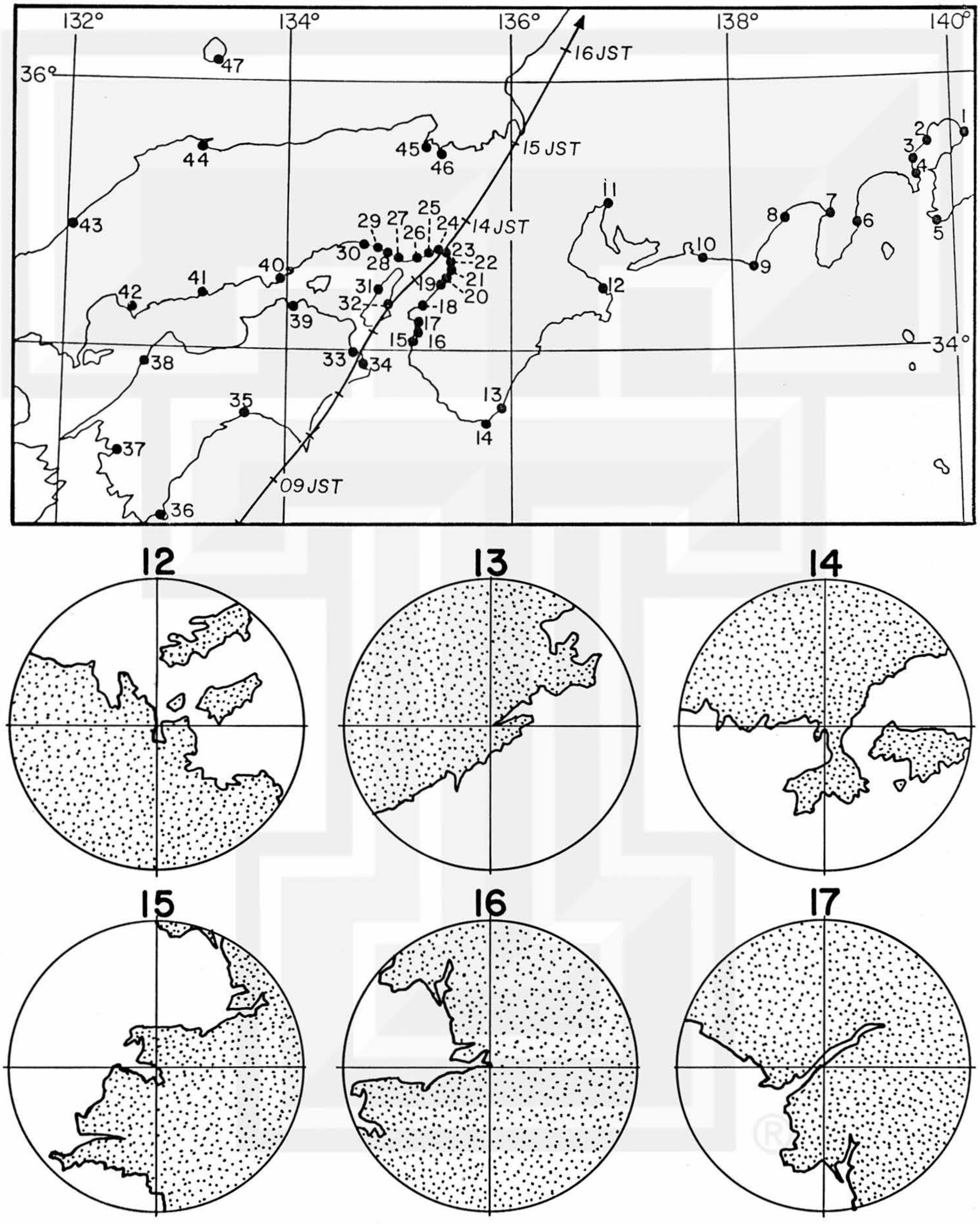

Fig. 3.3 Locations of tide-gage stations, 12-17.

Distribution of Tide-Gage Stations

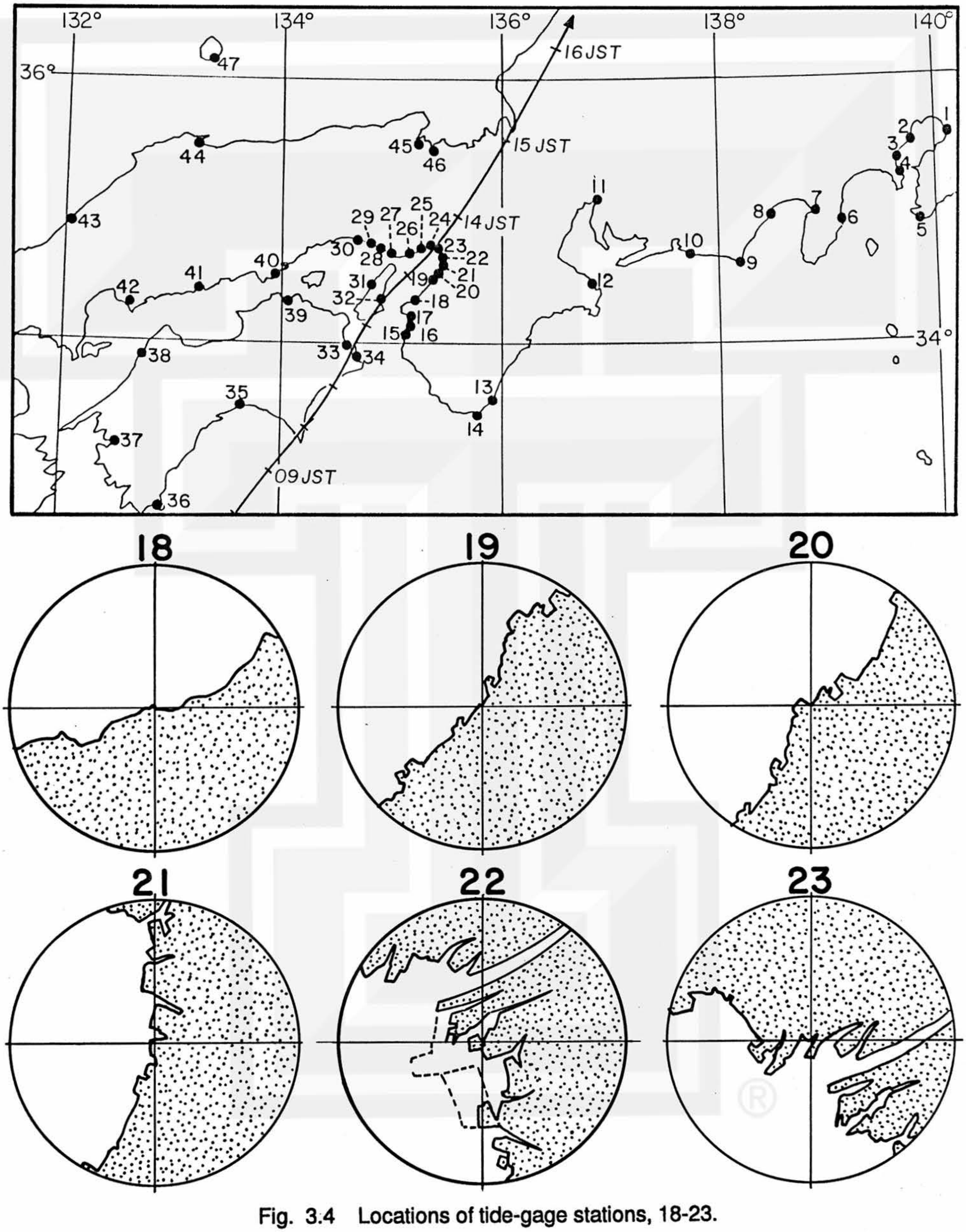

Fig. 3.4 Locations of tide-gage stations, 18-23.

Distribution of Tide-Gage Stations

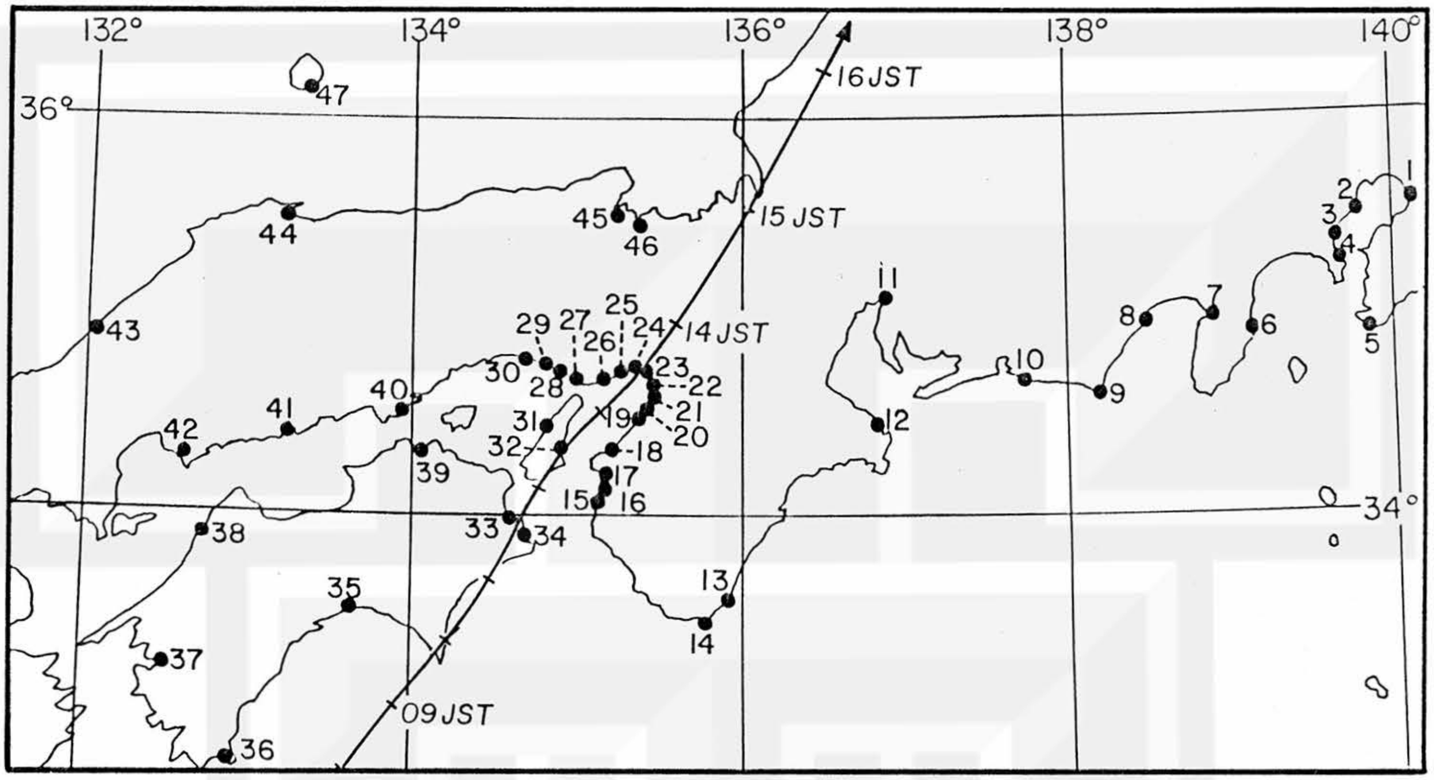

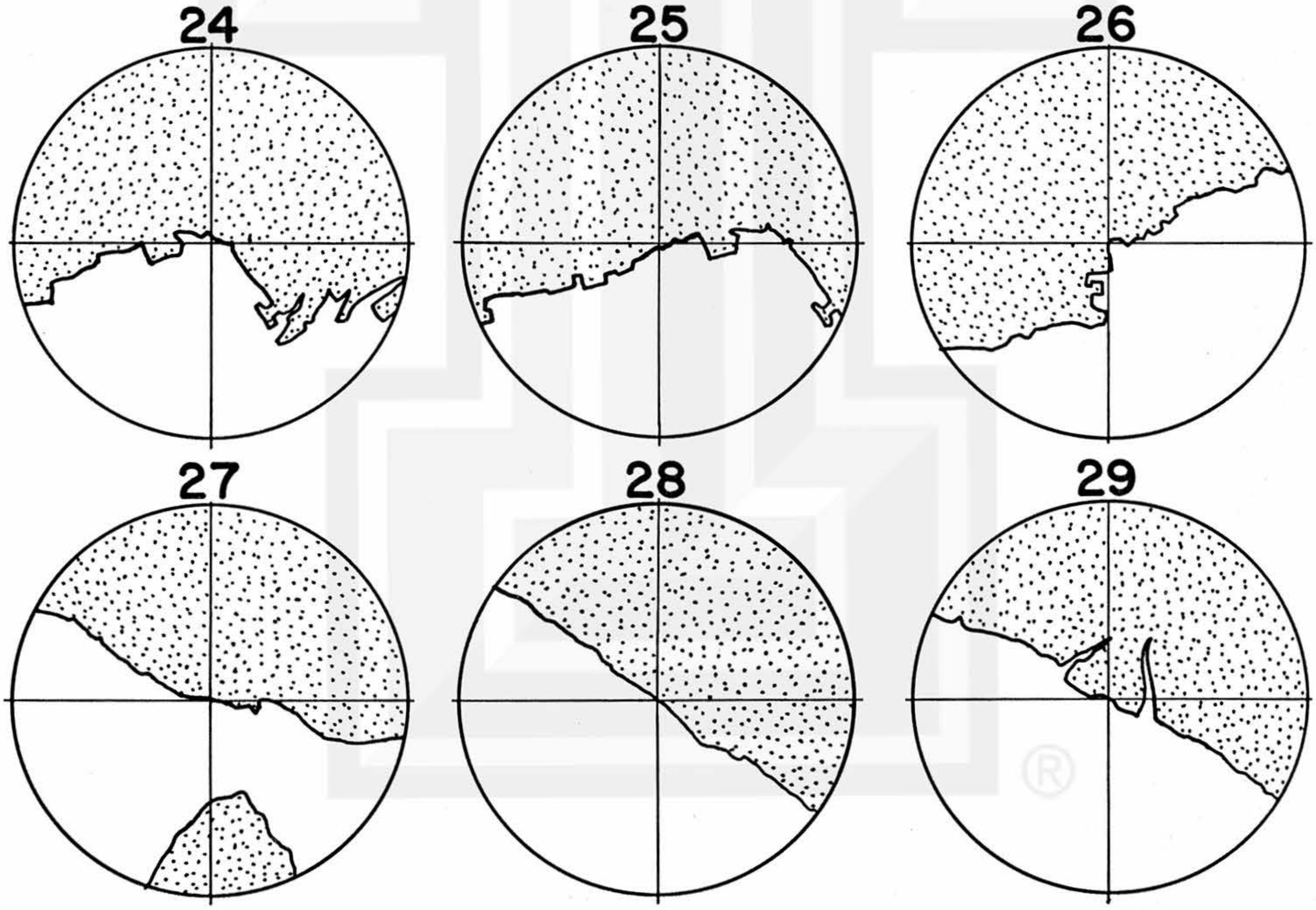

Fig. 3.5 Locations of tide-gage stations, 24-29.

Distribution of Tide-Gage Stations

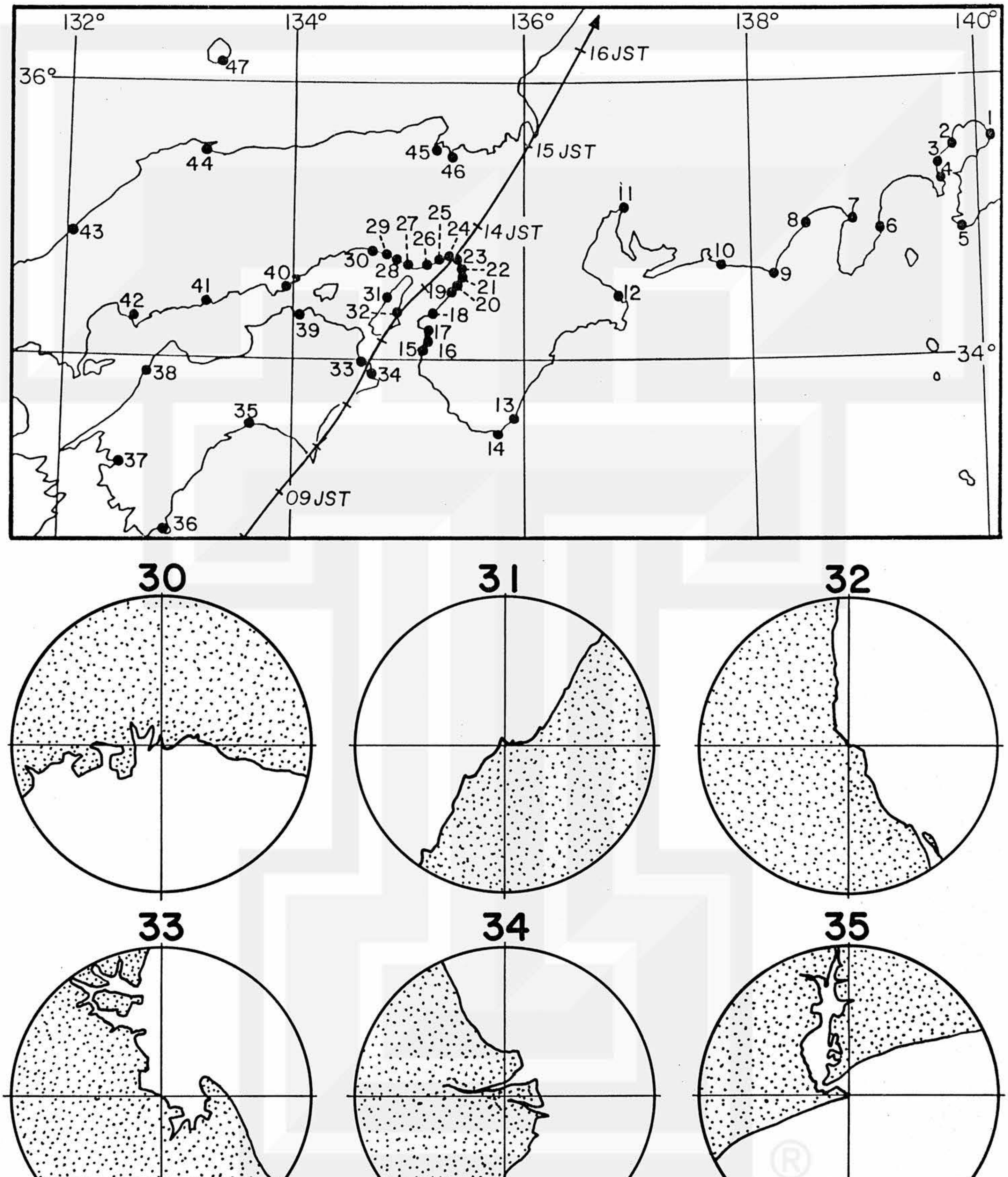

Fig. 3.6 Locations of tide-gage stations, 30-35.

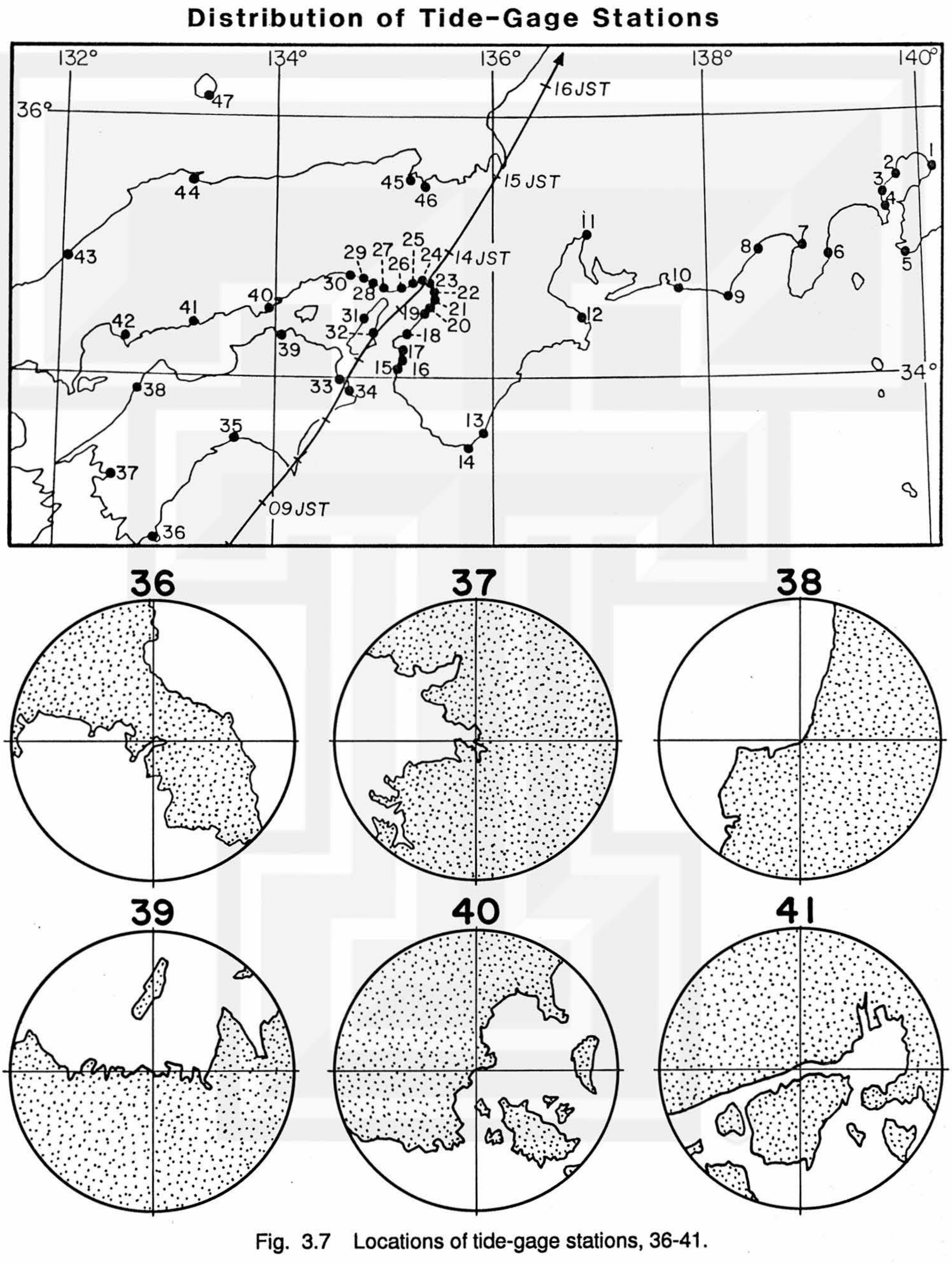

Fig. 3.7 Locations of tide-gage stations, 36-41.

Distribution of Tide-Gage Stations

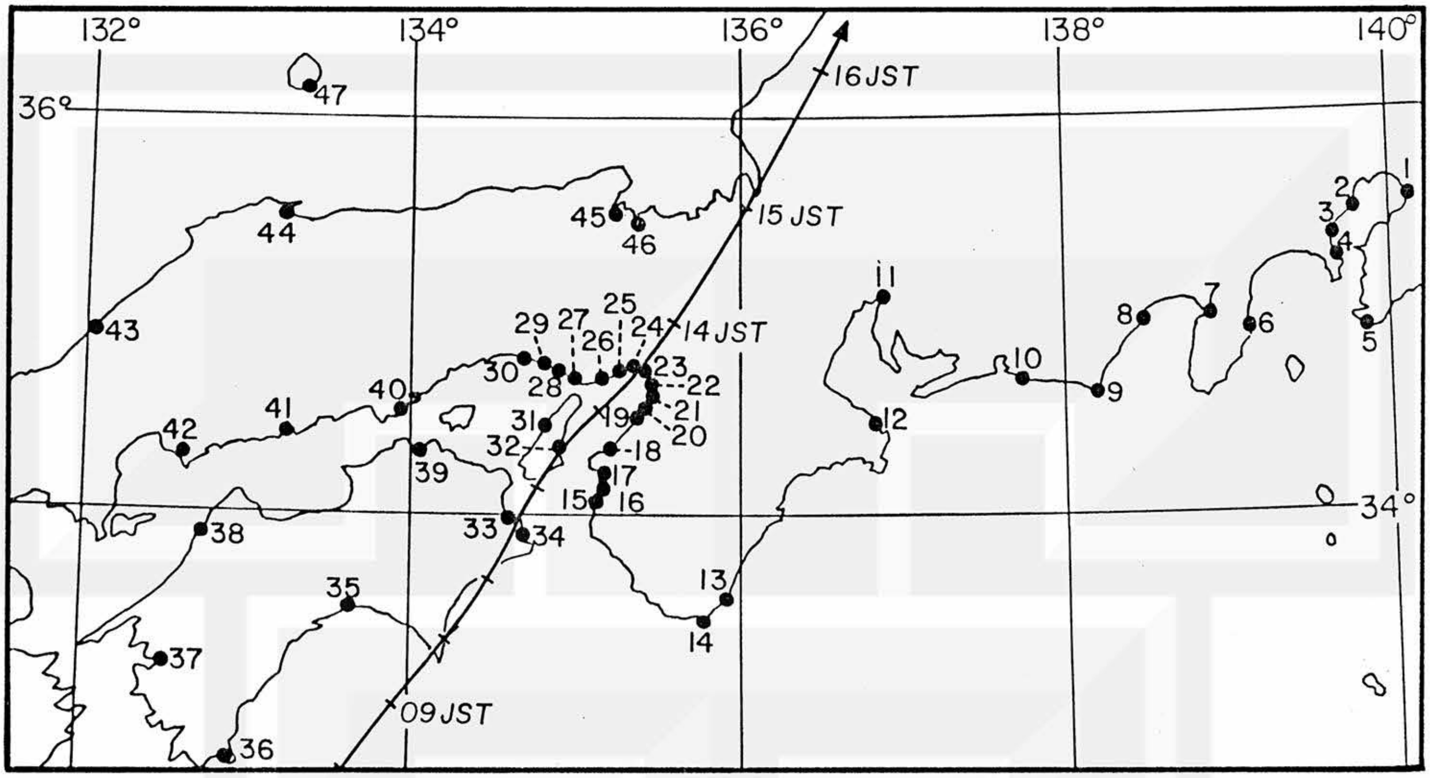

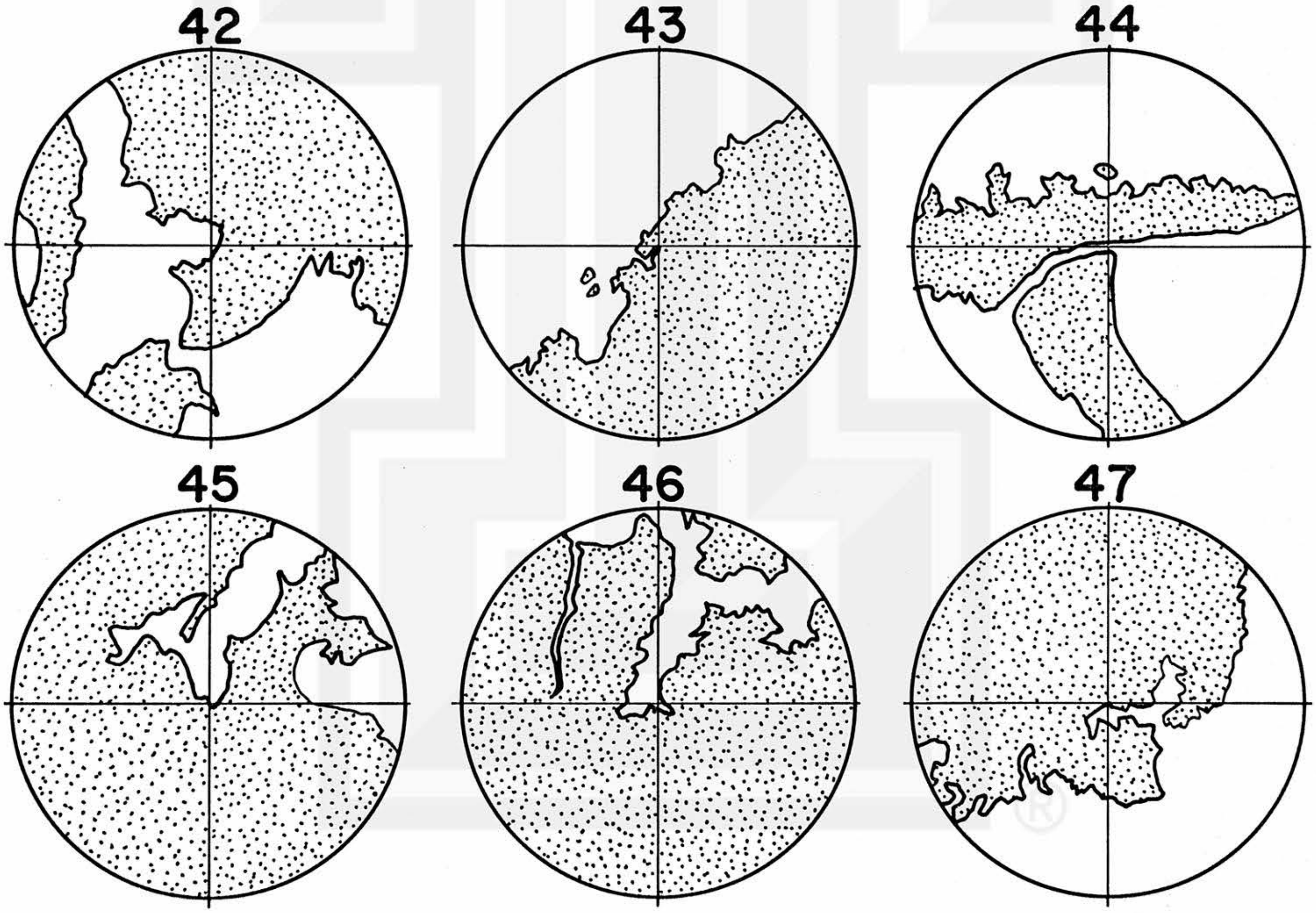

Fig. 3.8 Locations of tide-gage stations, 42-47.

4. SYNOPTIC-SCALE ANALYSIS

The tide-gage data presented in Section 3 covers most areas of the storm surge induced by Typhoon Nancy. The period of data tabulation is 7 hours, from 0900 JST to 1600 JST on 16 SEP 1961.

An attempt was made in this section to generate hourly synoptic-scale maps of the sea-level height anomalies for the data period. The typhoon moved from Tosa-bay to the Japan-sea coast during the seven-hour period.

The following series of hourly maps (see the top of each figure) includes the hourly isobaric map of Nancy analyzed and published in the JAM report. Shown beneath the isobaric maps are sea-level anomaly maps analyzed by Fujita. Data used are hourly anomalies at 47 tide-gage stations. Anomaly values at stations are shown in centimeters; 55 means 55 cm, -2 means negative 2 cm.

These anomaly values were contoured for every 10 cm. It is seen that a mound of high anomaly moved with the typhoon center while traveling over the open ocean (Fig. 4.1). Due to coastal influences the mound disappeared as the typhoon began crossing the coastline (Figs. 4.2 and 4.3) when high winds pushed the surface water against the coastline.

An interesting phenomenon found in Figures 4.4 and 4.5 was the piling up of surface water against a chain of islands, thus inducing a water pile which did not move with the typhoon. Such a pile-up is seen in Nagoya Bay (35°N and 137°E) and in Tokyo Bay (35°N and 140°E), far away locations from the typhoon center (Figs. 4.6 - 4.8).

It is of interest to see that piles of water did not recede for a long time after the passage of the typhoon center, due mainly to the stress of onshore winds which kept pushing the surface water deep into the bays. At 1400 JST, the pile in Osaka Bay (35°N and 135°E) became very pronounced - a 236 cm anomally.

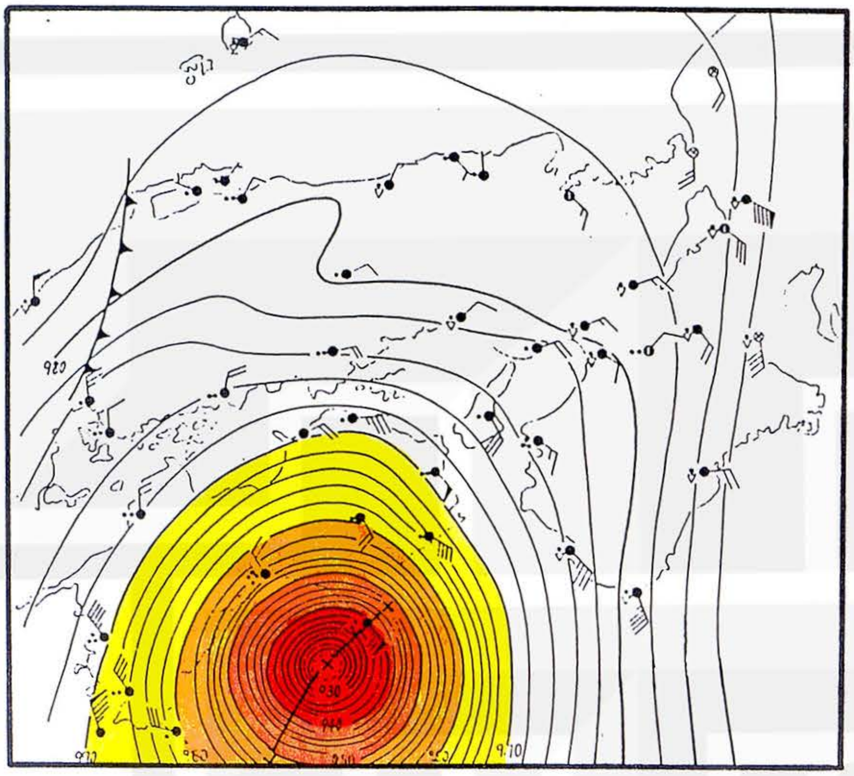

Typhoon Nancy of
16 SEP 1961

0900 JST

Map by JMA

Sea-level Height Anomaly (cm) at Surface-map Time

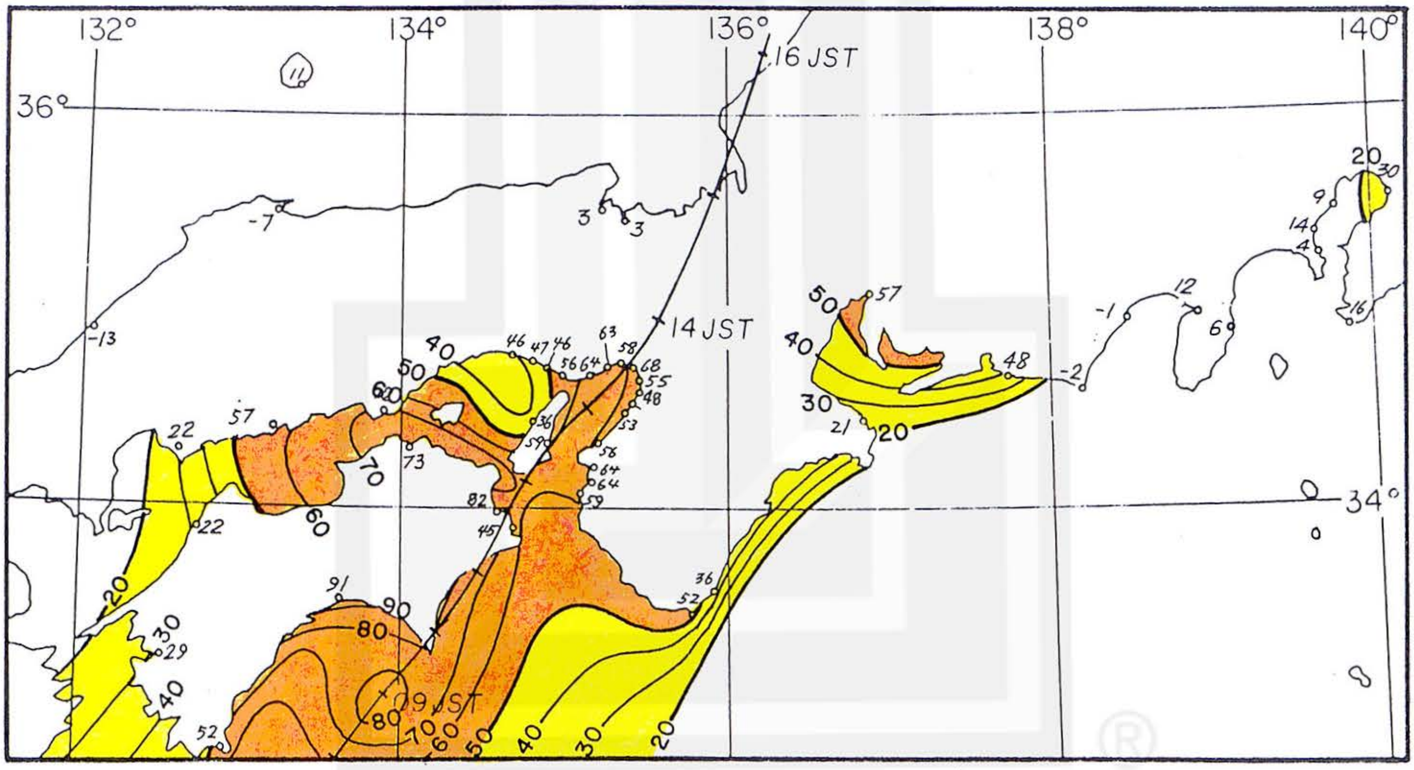

Fig. 4.1 Sea-level height anomaly at 0900 JST, 16 SEP 1961.

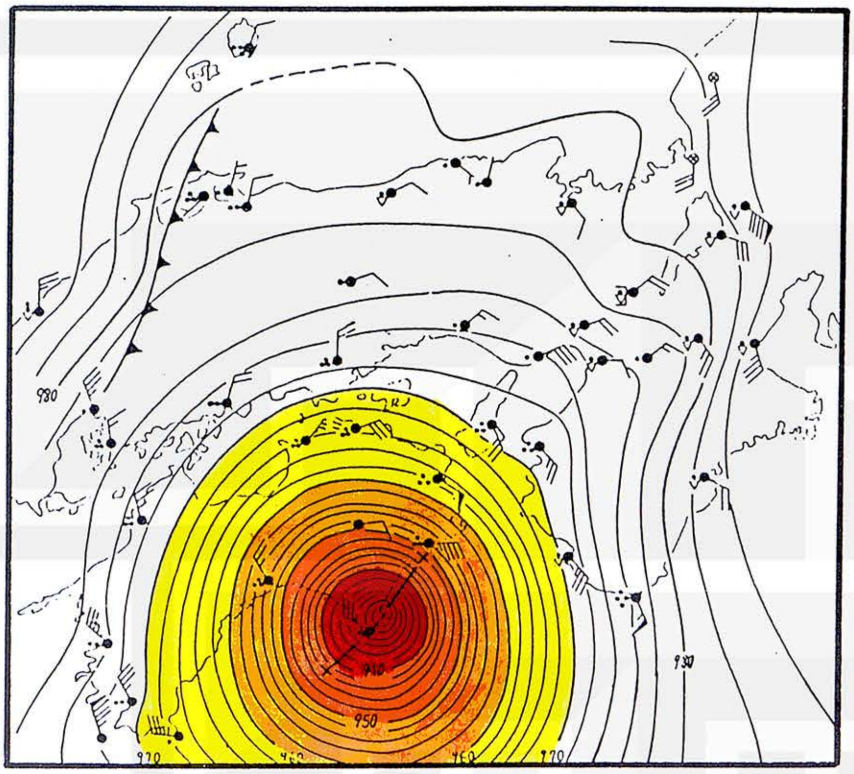

Typhoon Nancy of
16 SEP 1961

1000 JST

Map by JMA

Sea-level Height Anomaly (cm) at Surface-map Time

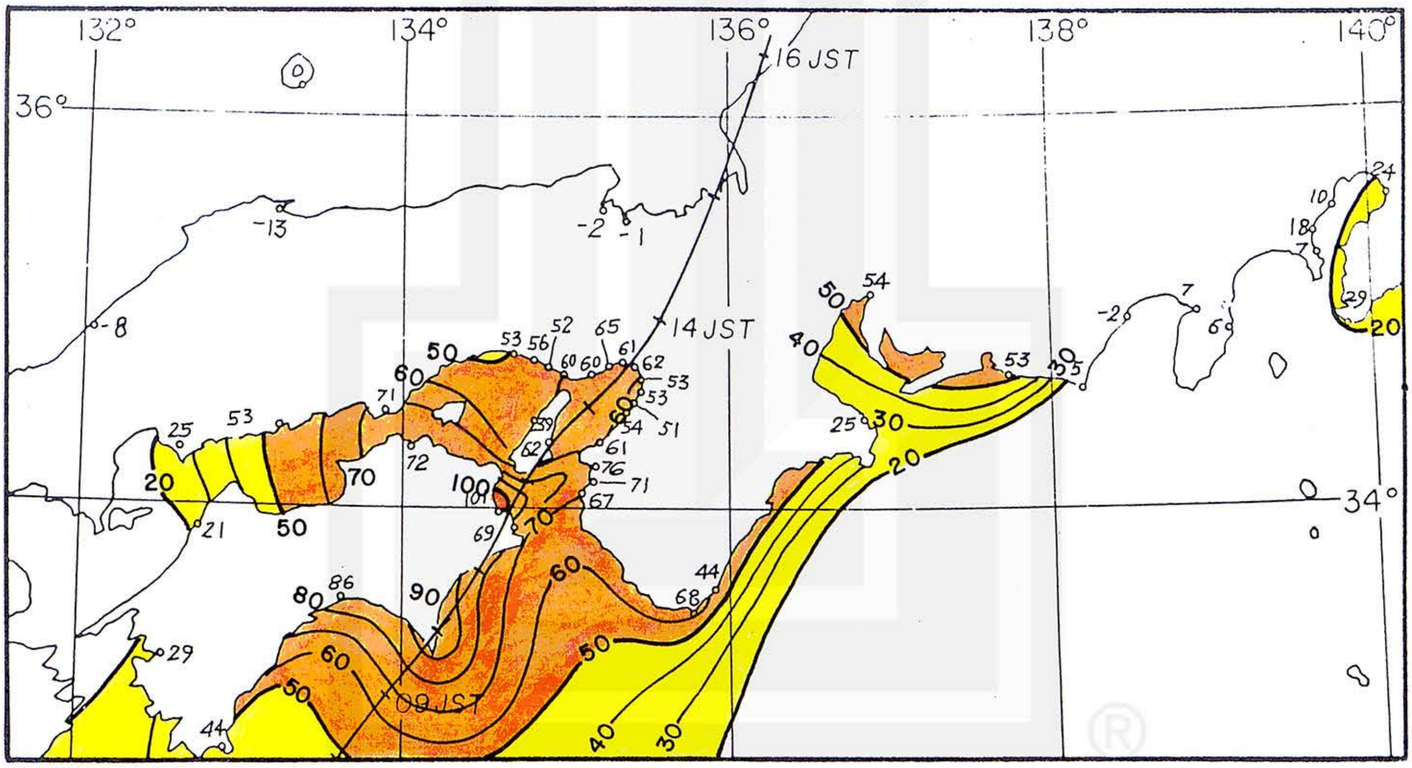

Fig. 4.2 Sea-level height anomaly at 1000 JST, 16 SEP 1961.

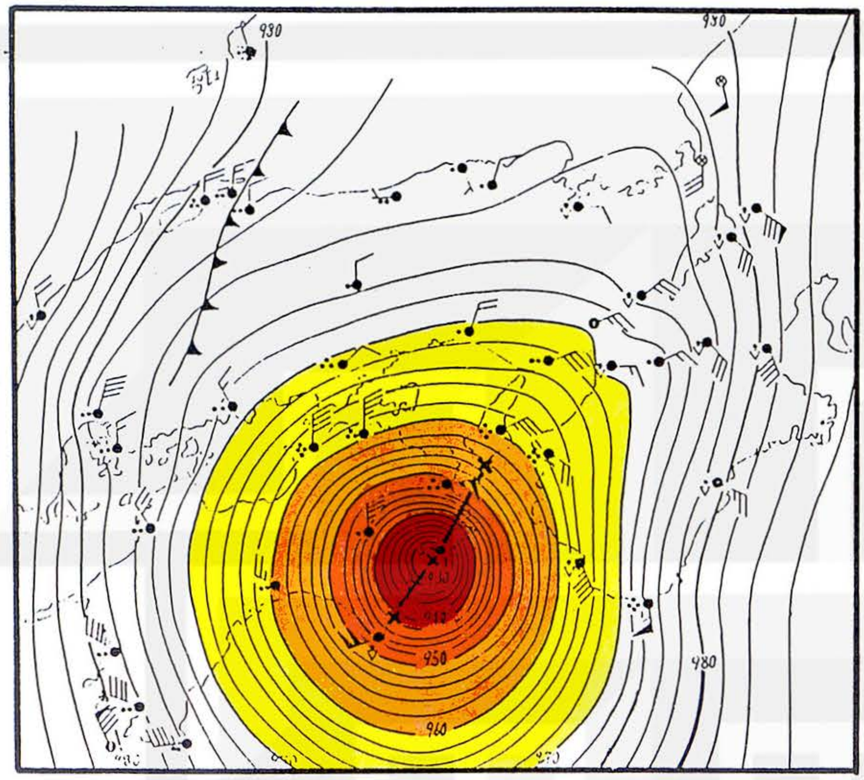

Typhoon Nancy of
16 SEP 1961

1100 JST

Map by JMA

Sea-level Height Anomaly (cm) at Surface-map Time

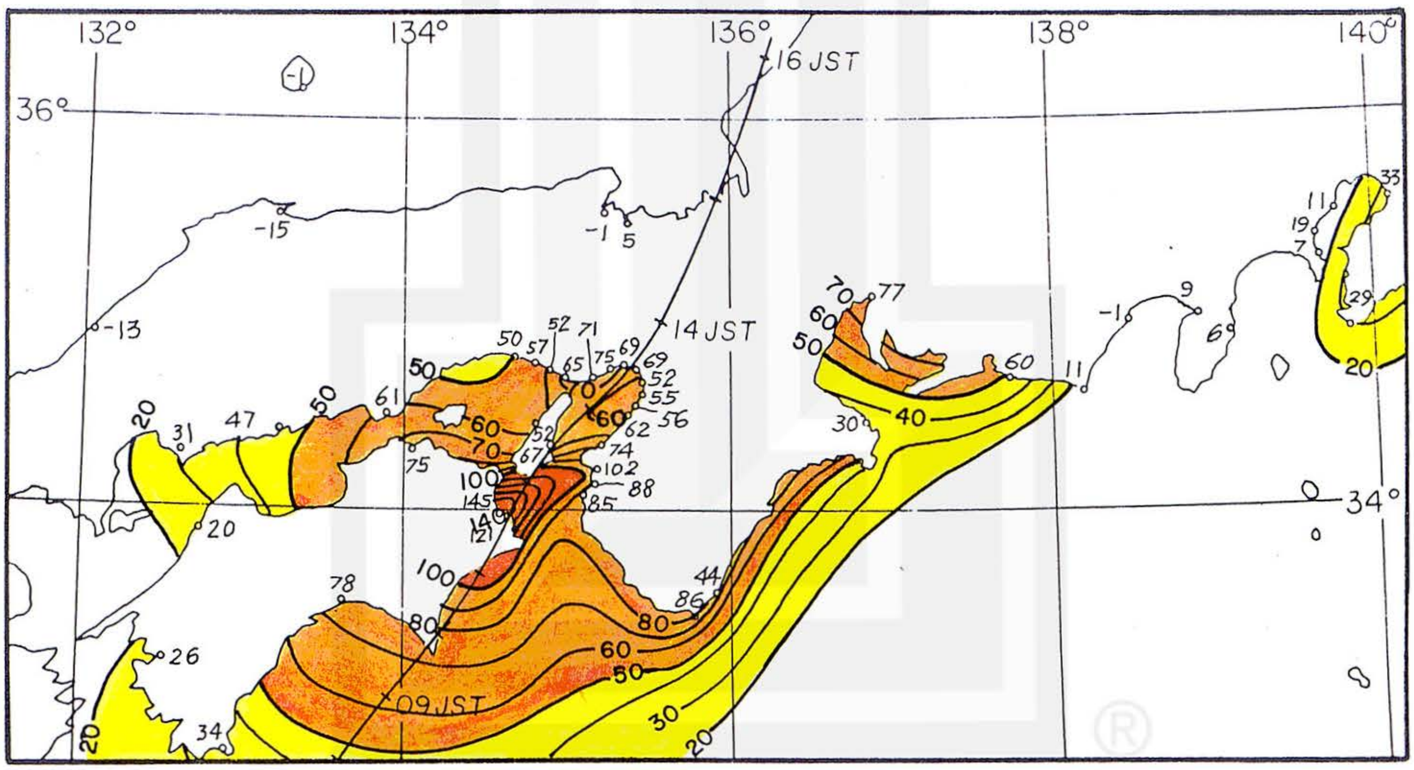

Fig. 4.3 Sea-level height anomaly at 1100 JST, 16 SEP 1961.

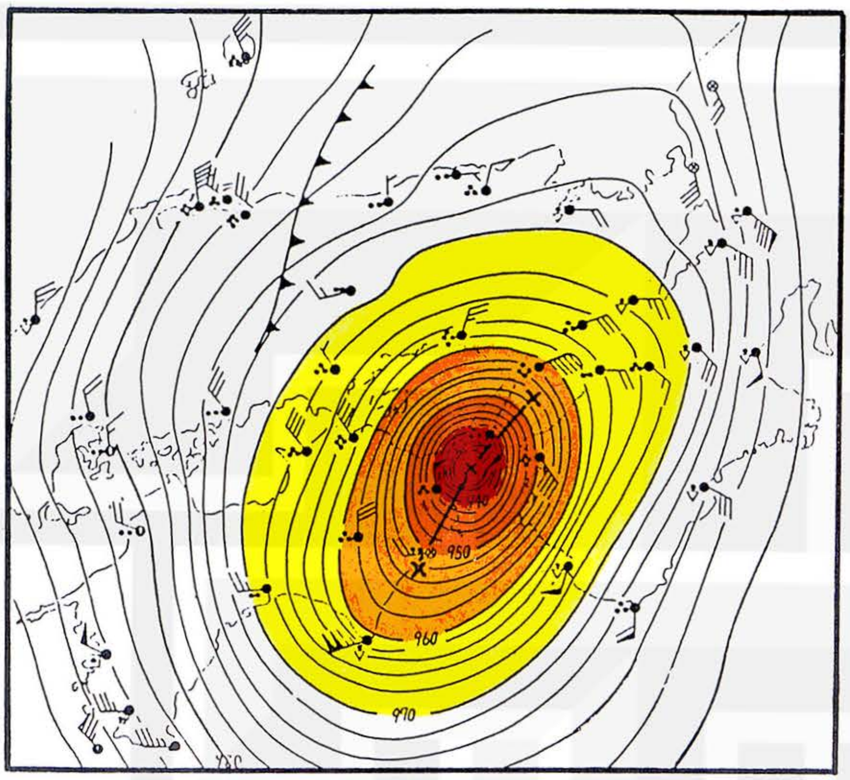

Typhoon Nancy of

16 SEP 1961

1200 JST

Map by JMA

Sea-level Height Anomaly (cm) at Surface-map Time

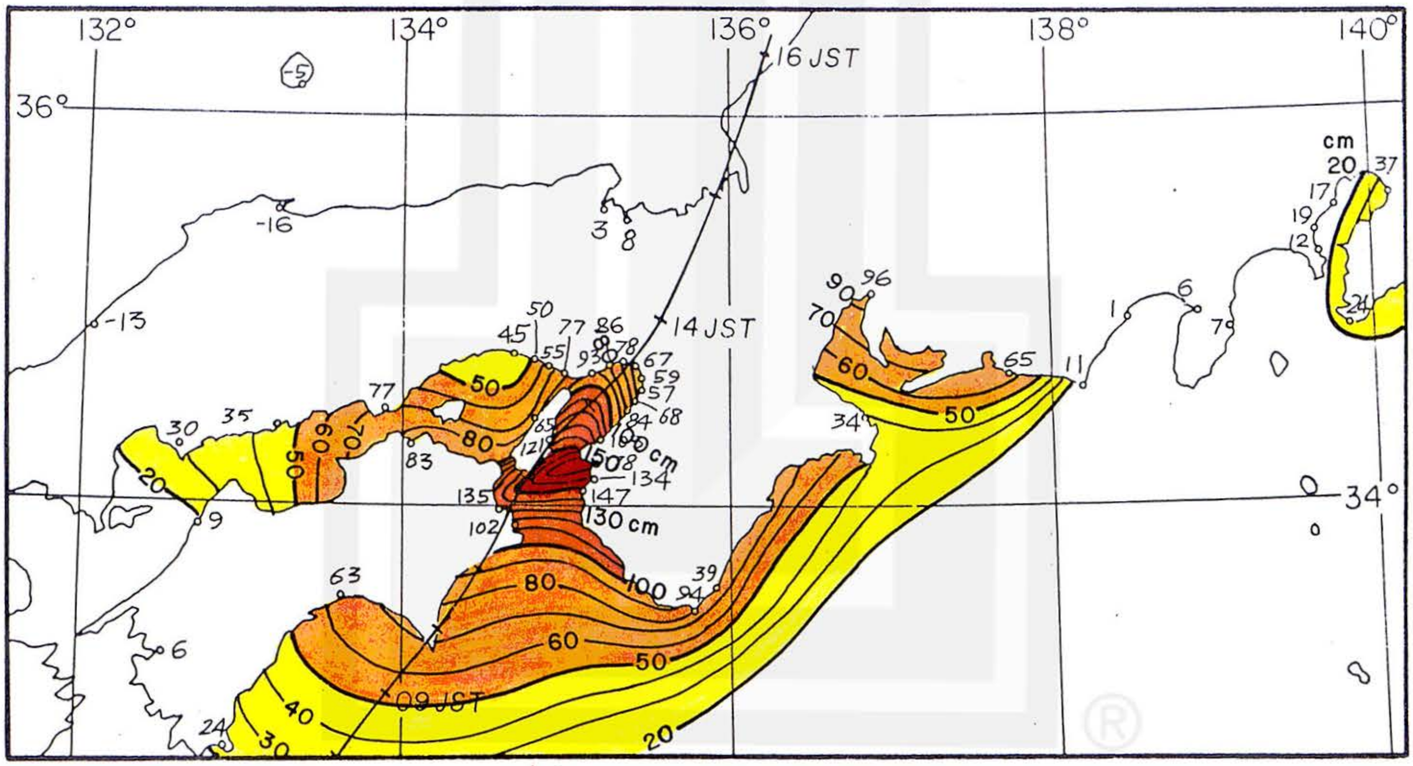

Fig. 4.4 Sea-level height anomaly at 1200 JST, 16 SEP 1961.

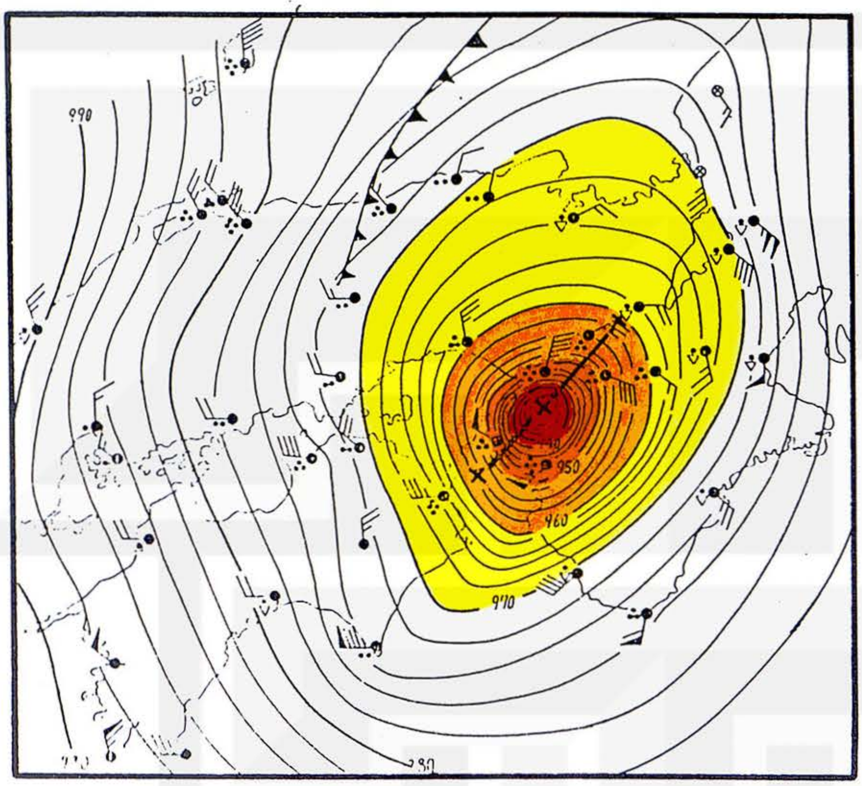

Typhoon Nancy of
16 SEP 1961

1300 JST

Map by JMA

Sea-level Height Anomaly (cm) at Surface-map Time

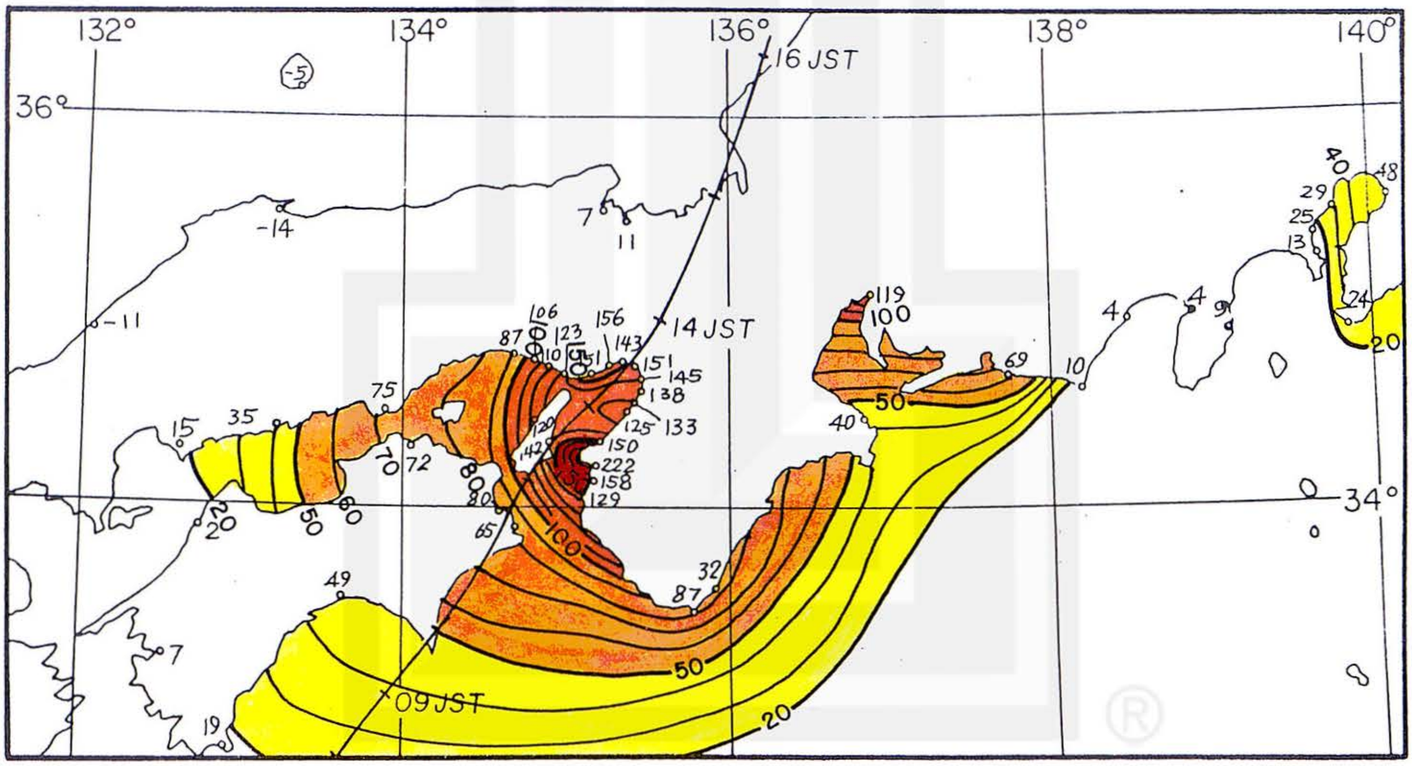

Fig. 4.5 Sea-level height anomaly at 1300 JST, 16 SEP 1961.

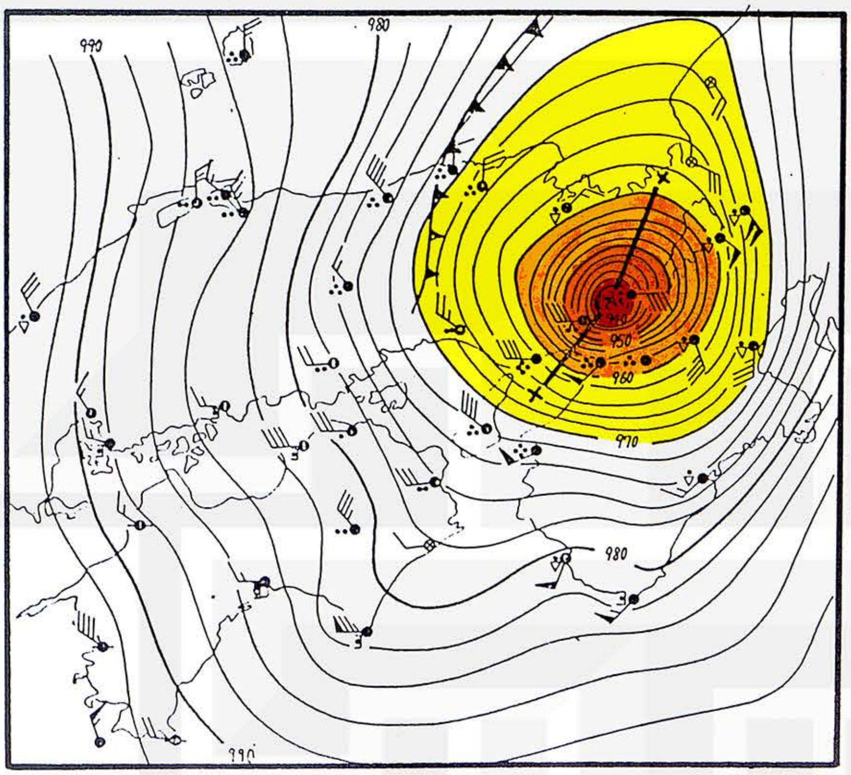

Typhoon Nancy of 16 SEP 1961

1400 JST

Map by JMA

Sea-level Height Anomaly (cm) at Surface-map Time

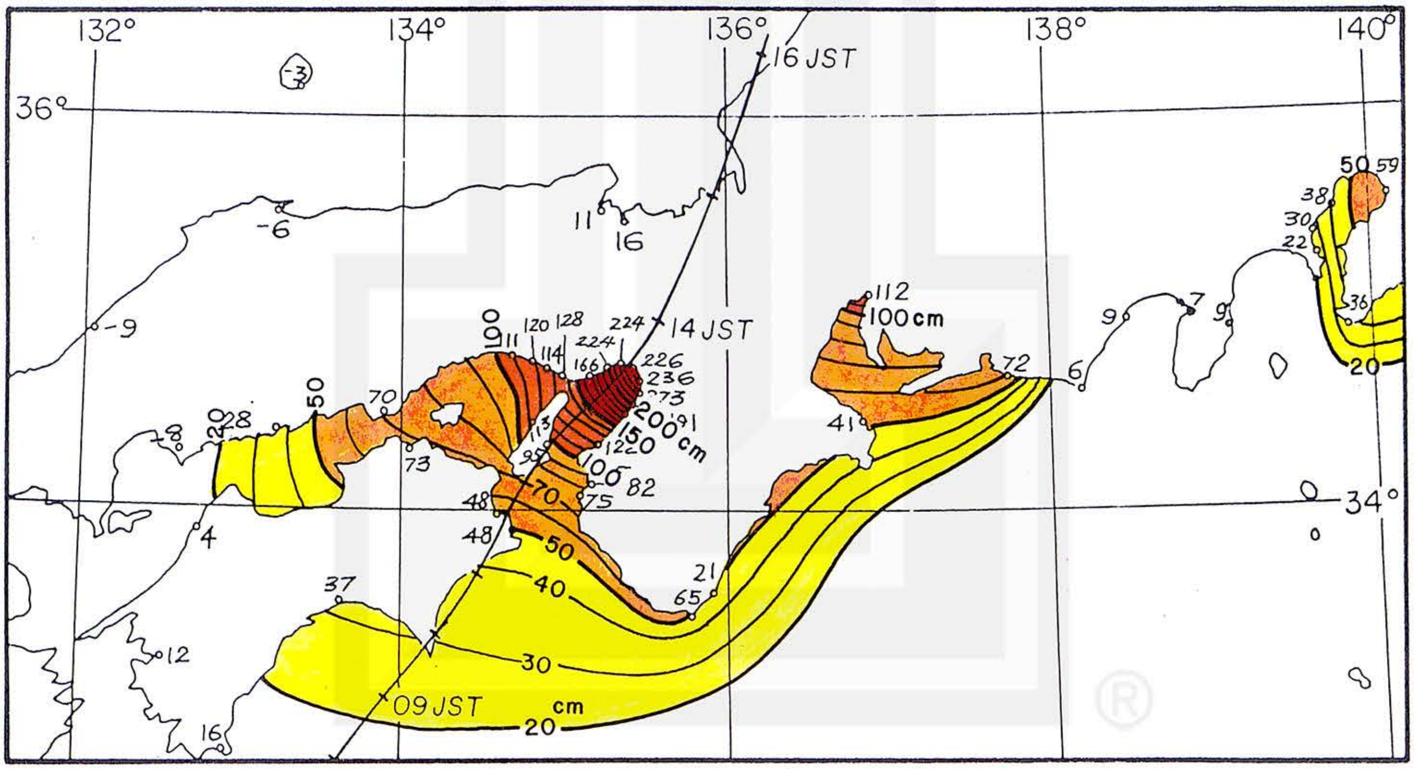

Fig. 4.6 Sea-level height anomaly at 1400 JST, 16 SEP 1961.

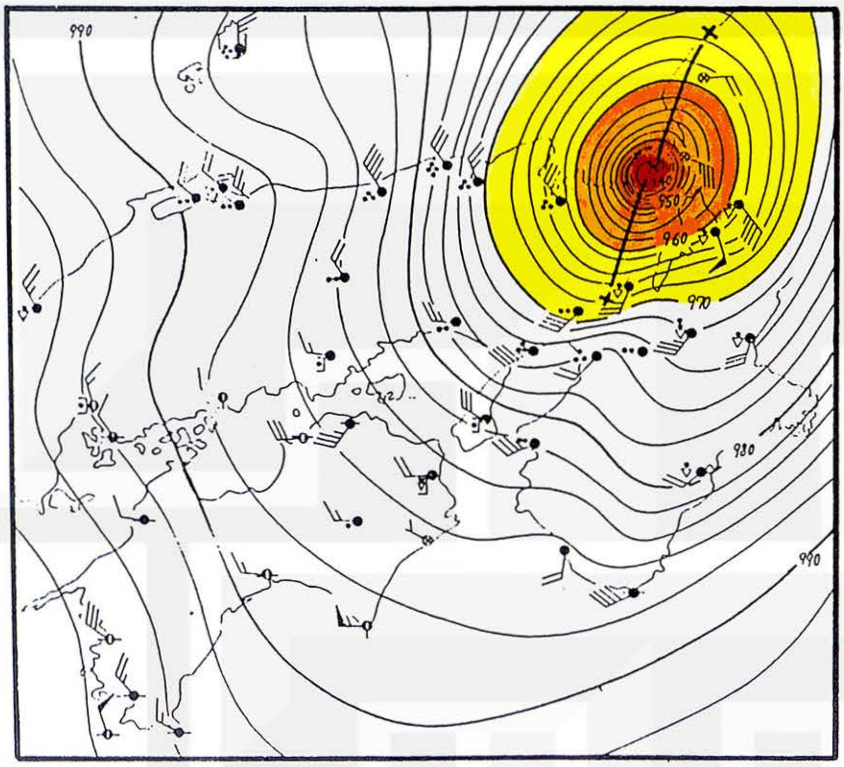

Typhoon Nancy of
16 SEP 1961

1500 JST

Map by JMA

Sea-level Height Anomaly (cm) at Surface-map Time

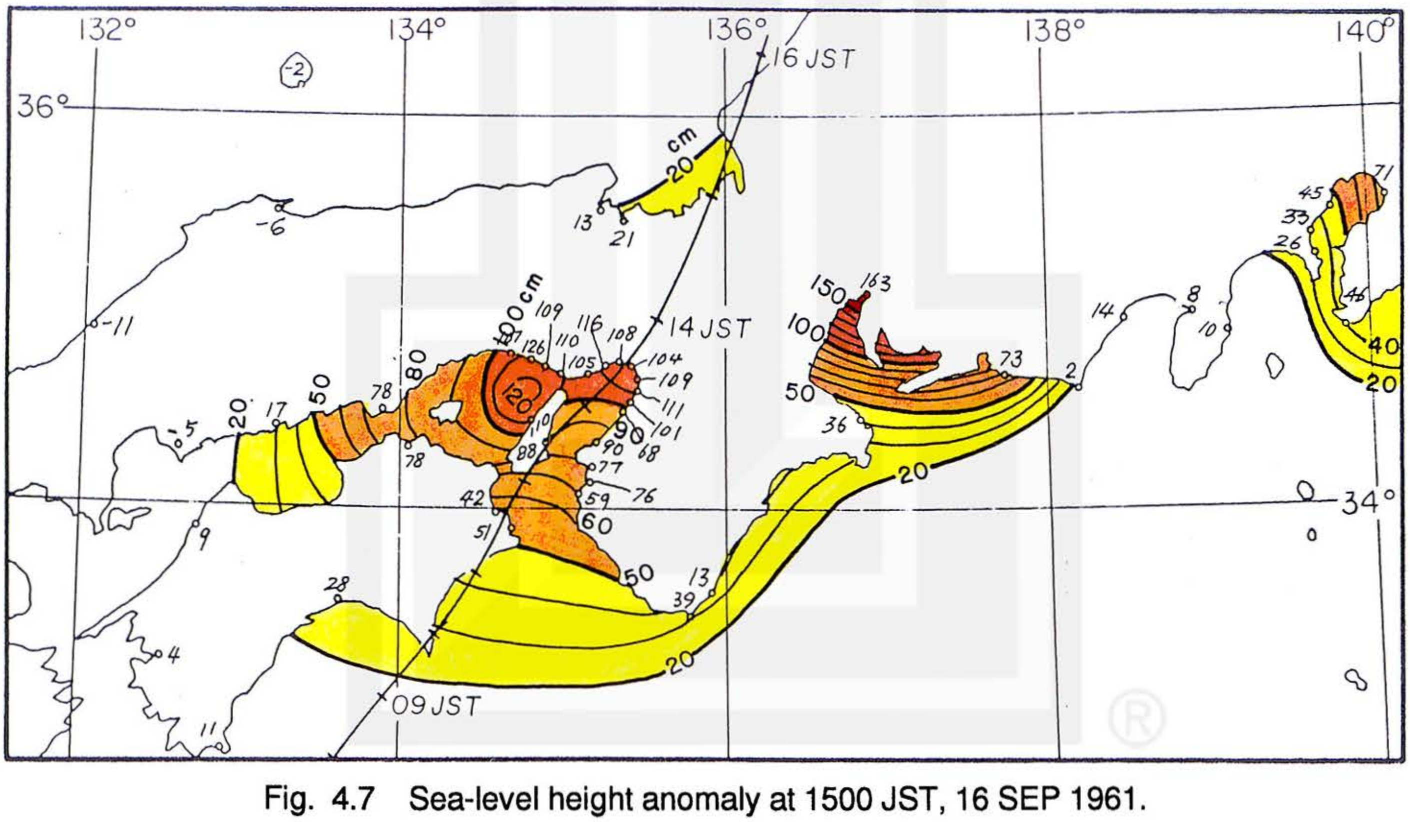

Fig. 4.7 Sea-level height anomaly at 1500 JST, 16 SEP 1961.

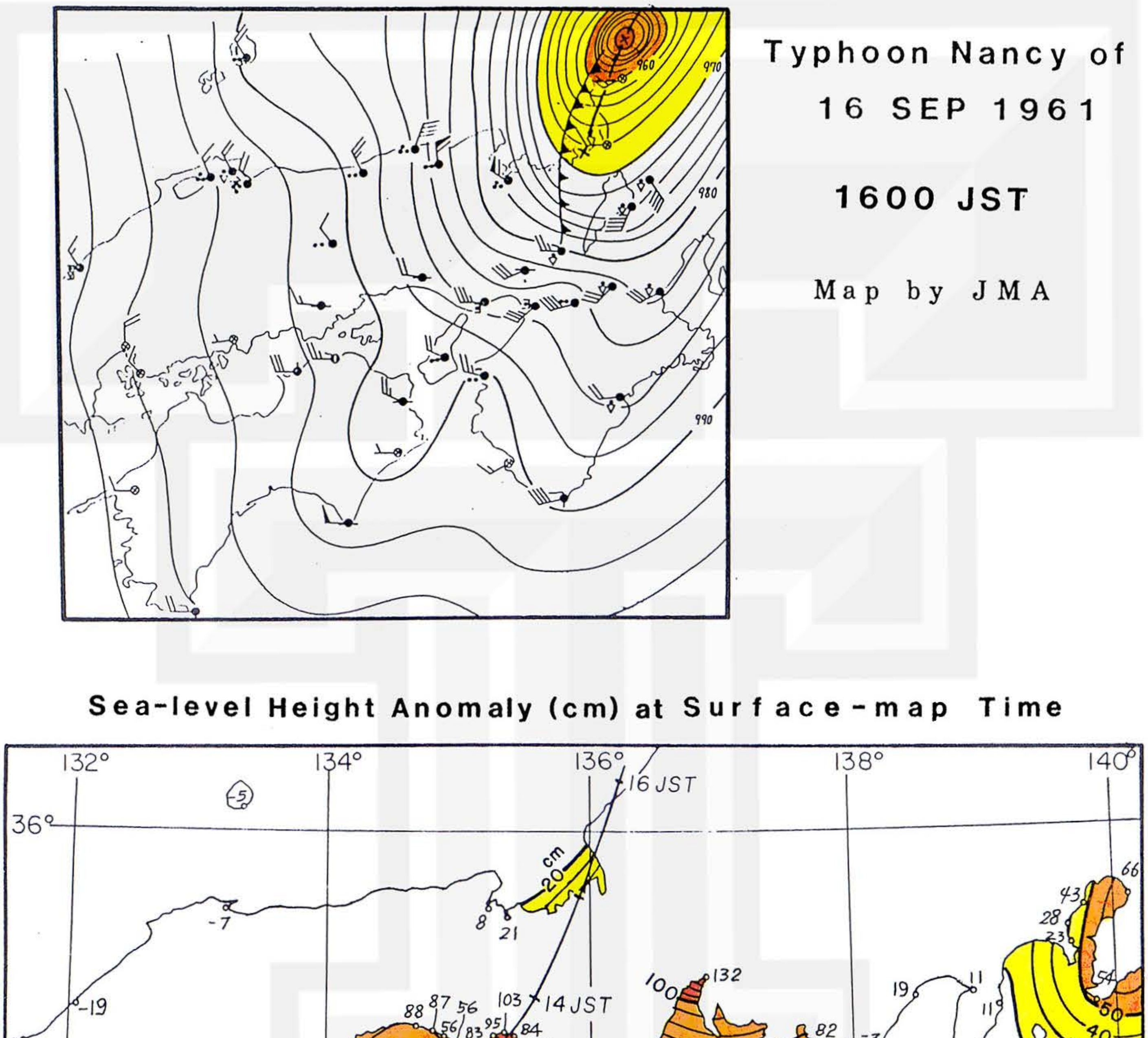

Fig. 4.8 Sea-level height anomaly at 1600 JST, 16 SEP 1961.

5. MESOSCALE SURGE IN BAYS AND INLETS

Typhoon Nancy crossed the islands of Japan diagonally from southwest to northeast passing between Kobe and Osaka (Fig. 5.1). There are numerous small bays and inlets which responded differently to the wind and pressure fields of the violent typhoon. Because the water areas are so complicated, a sequence of mesoscale analyses at 10 to 60 minute intervals became necessary.

Due to the fact that sea-level anomalies are caused by the combined effects of pressure and wind, tide-gage stations around Osaka Bay recorded several peak heights which propagated northward (Fig. 5.2). The most significantanomaly was Surge 2 which propagated at 45 mph, from Station 18 to Station 26 in one hour. The peak time of Surge 2 was 20 to 40 minutes behind the minimum pressure time, suggesting that the peak surge took place during the strong onshore winds on the back side of the typhoon center.

At 1100 JST, the storm center was located near the eastern tip of Shikoku. Strong southerly winds over the Kii Channel were transporting surface water toward Awaji Island. Two narrows on the east and west sides of the island were not wide enough, resulting in a water pile-up on the south side of the island. At 1200 JST the pile became significant, reaching over 180 cm in the Tomogashima Narrows (Fig. 5.4). When the typhoon center moved northeast, parallel to the coast, strong southwest winds blew against the 10 mile long coastline northwest of Wakayama. The Wakayama tide gage registered an estimated 345 cm anomaly (Fig. 5.5). Thereafter, the typhoon center moved northeast. The Wakayama anomaly did not move into Osaka Bay because the Tomogashima Narrows did not allow the passage of water into Osaka Bay.

By 1320 JST, the typhoon center moved toward the northeast shore of Osaka Bay. The anomaly at Station 21 was only 125 cm because of the strong offshore winds. On the other hand, strong onshore winds pushed water against the coastline between stations 20 and 21 (Fig. 5.6). This situation continued through 1340 JST (Figs. 5.7 and 5.8).

Thereafter, the wind direction at the northeast end of Osaka Bay changed from west-southwest to southwest, stimulating the pile of water against the northeast coast of Osaka Bay long after the typhoon center moved inland toward the city of Kyoto (Figs. 5.9 and 5.10).

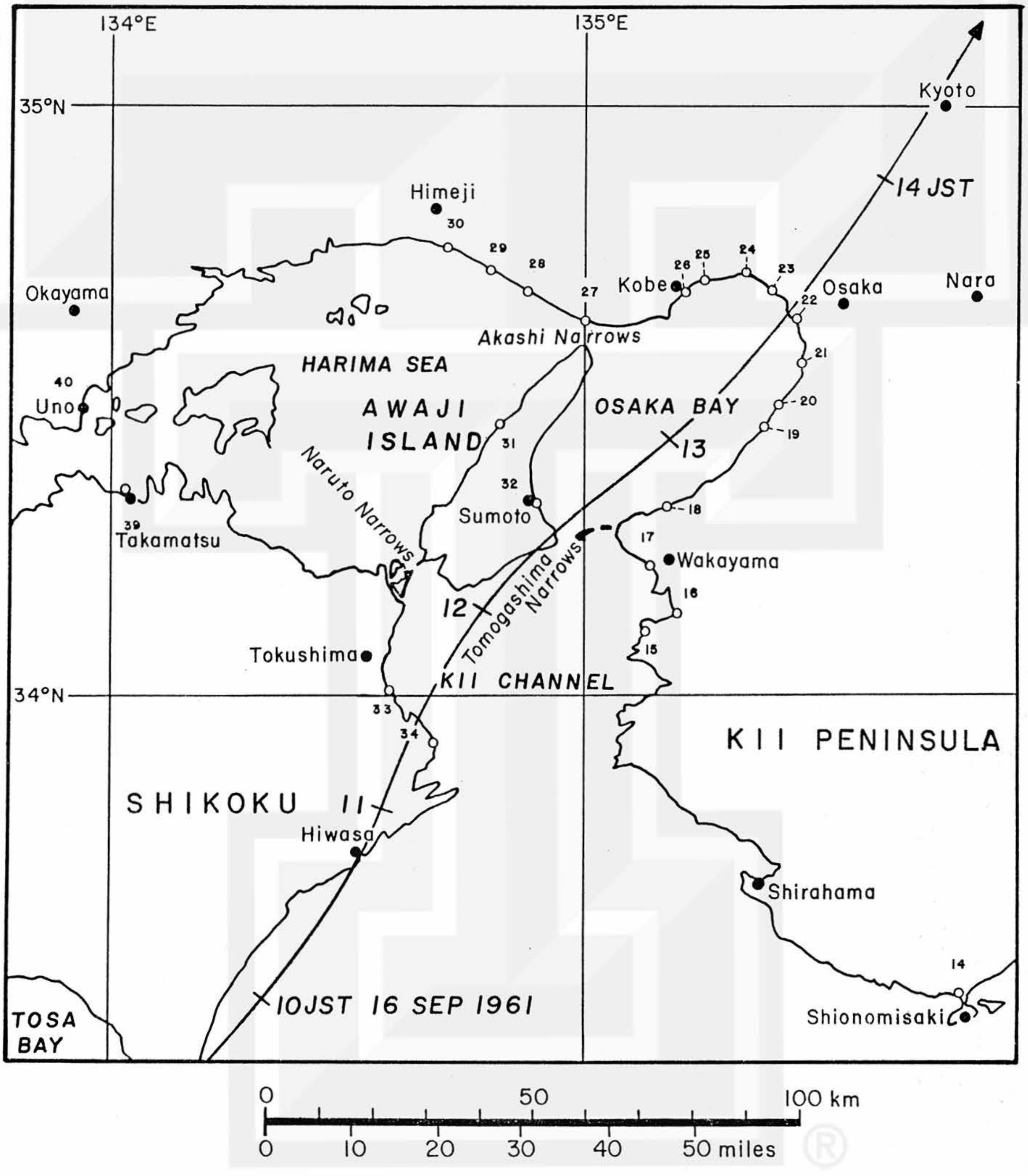

Fig. 5.1 Local map of the storm surge area analyzed by the mesoanalysis technique developed by Fujita.

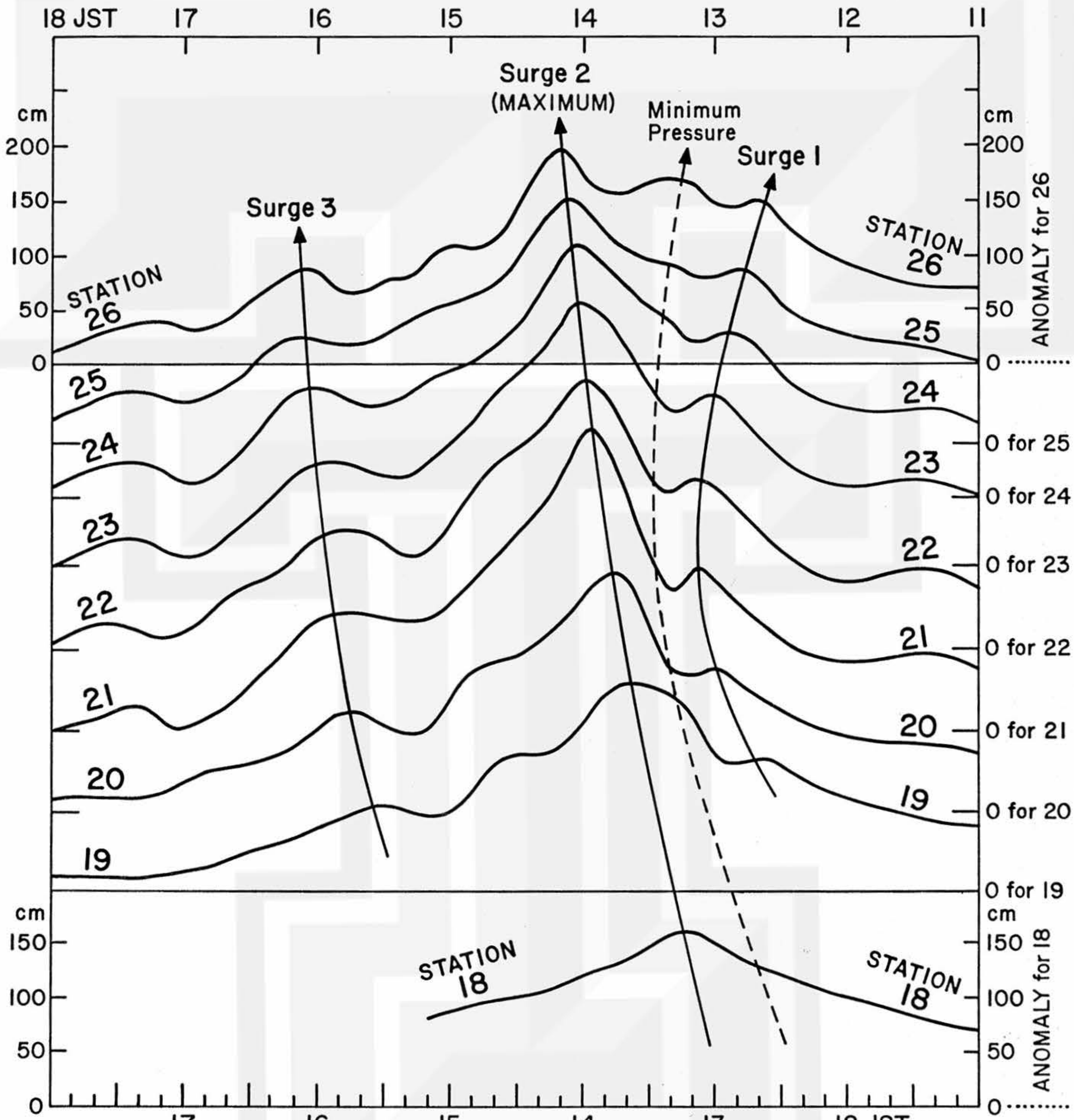

Fig. 5.2 Progression of the surge height detected by tide-gage stations 18 through 26 as it moved along the coast of Osaka Bay (see the local map for identifying locations).

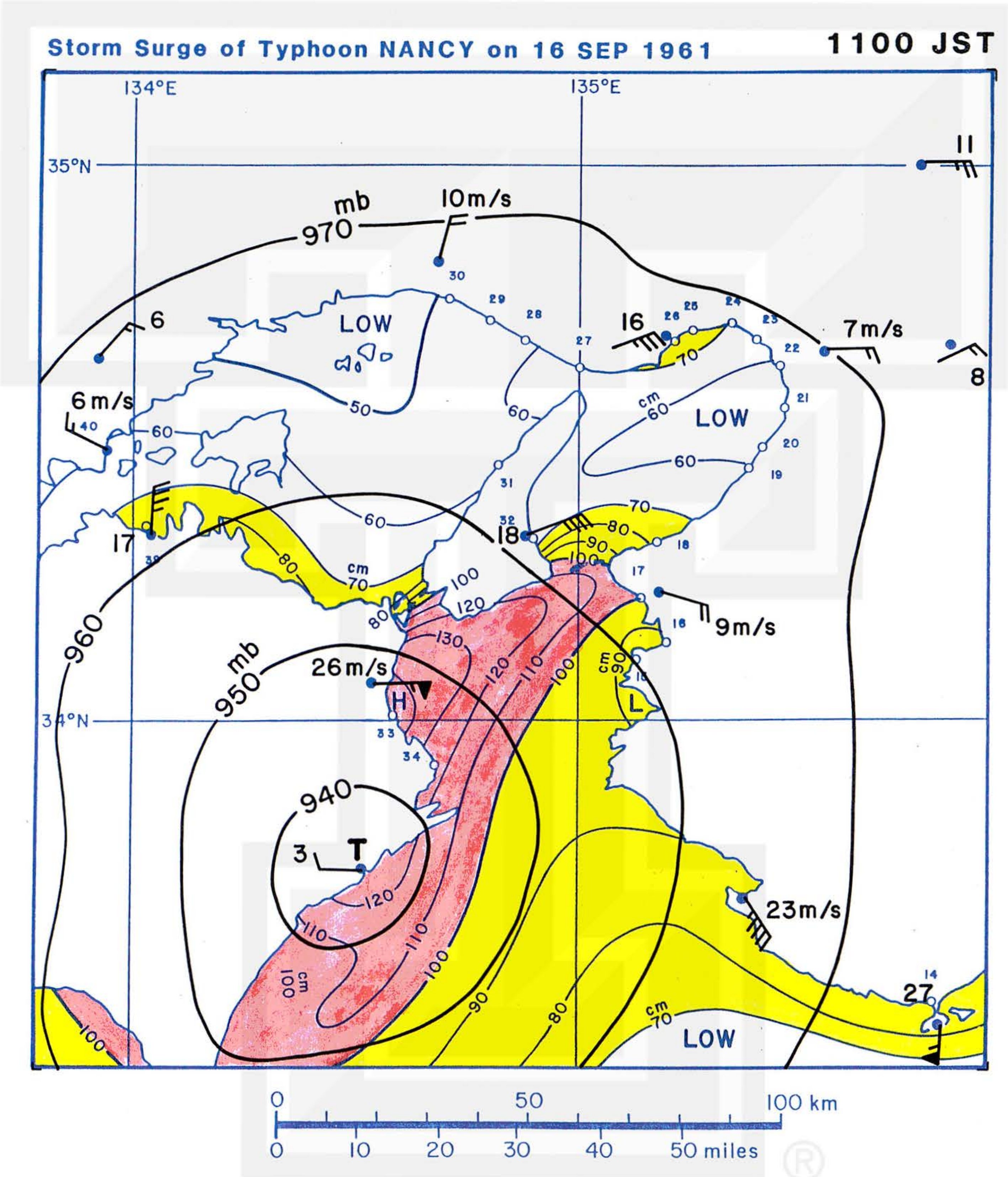

Fig. 5.3 Pattern of sea-level height anomalies at 1100 JST, 16 SEP 1961.

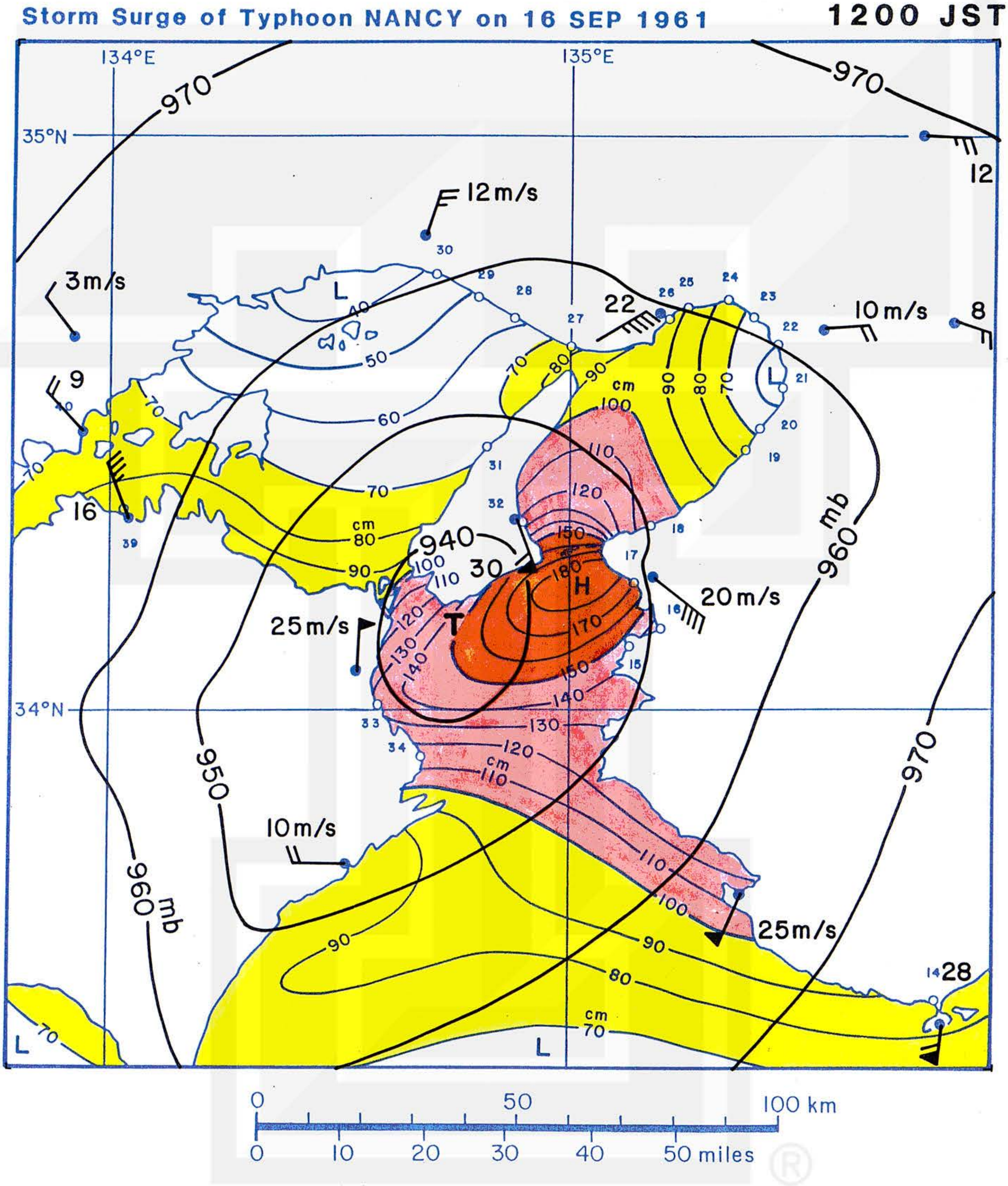

Fig. 5.4 Pattern of sea-level height anomalies at 1200 JST, 16 SEP 1961.

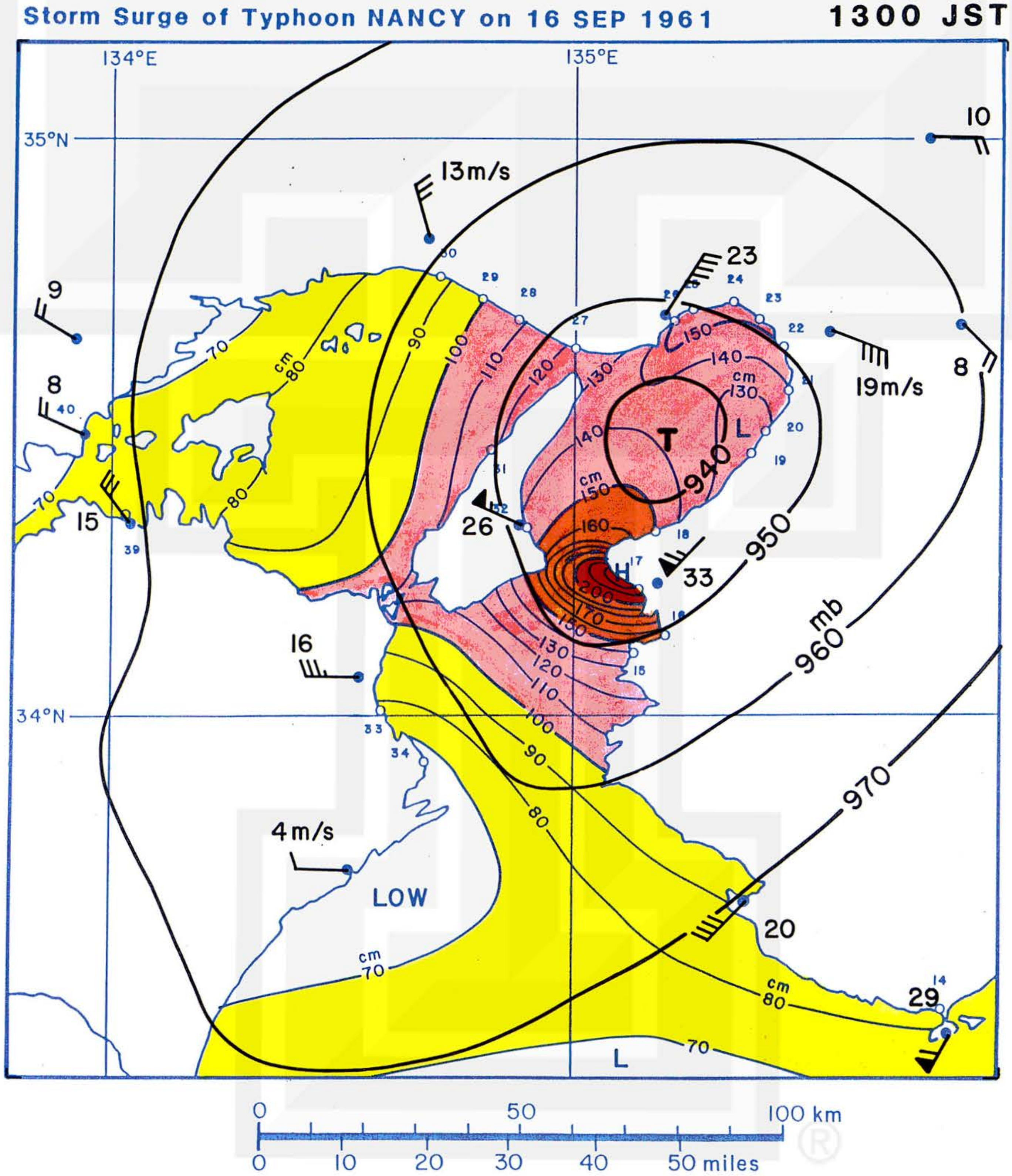

Fig. 5.5 Pattern of sea-level height anomalies at 1300 JST, 16 SEP 1961.

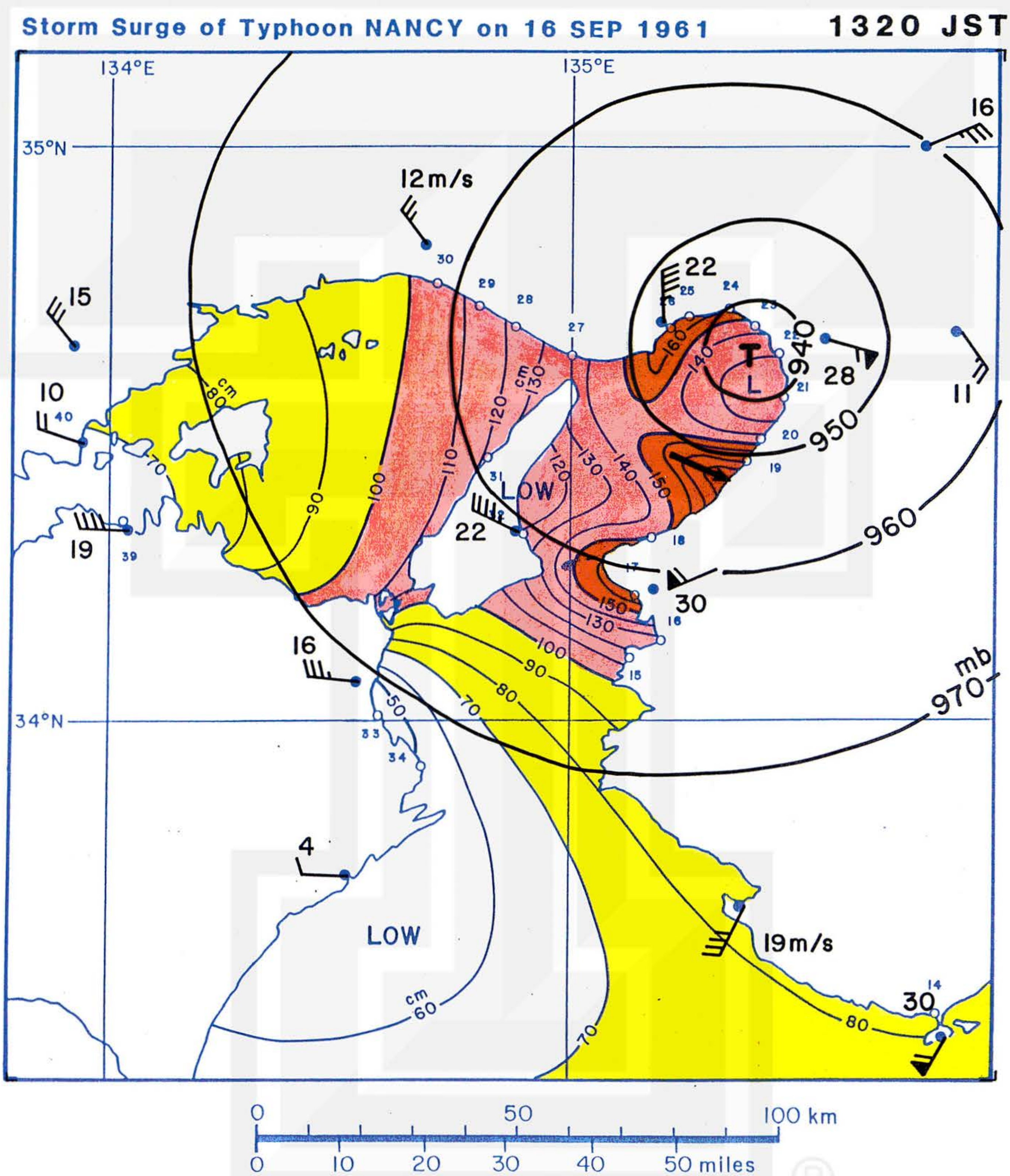

Fig. 5.6 Pattern of sea-level height anomalies at 1320 JST, 16 SEP 1961.

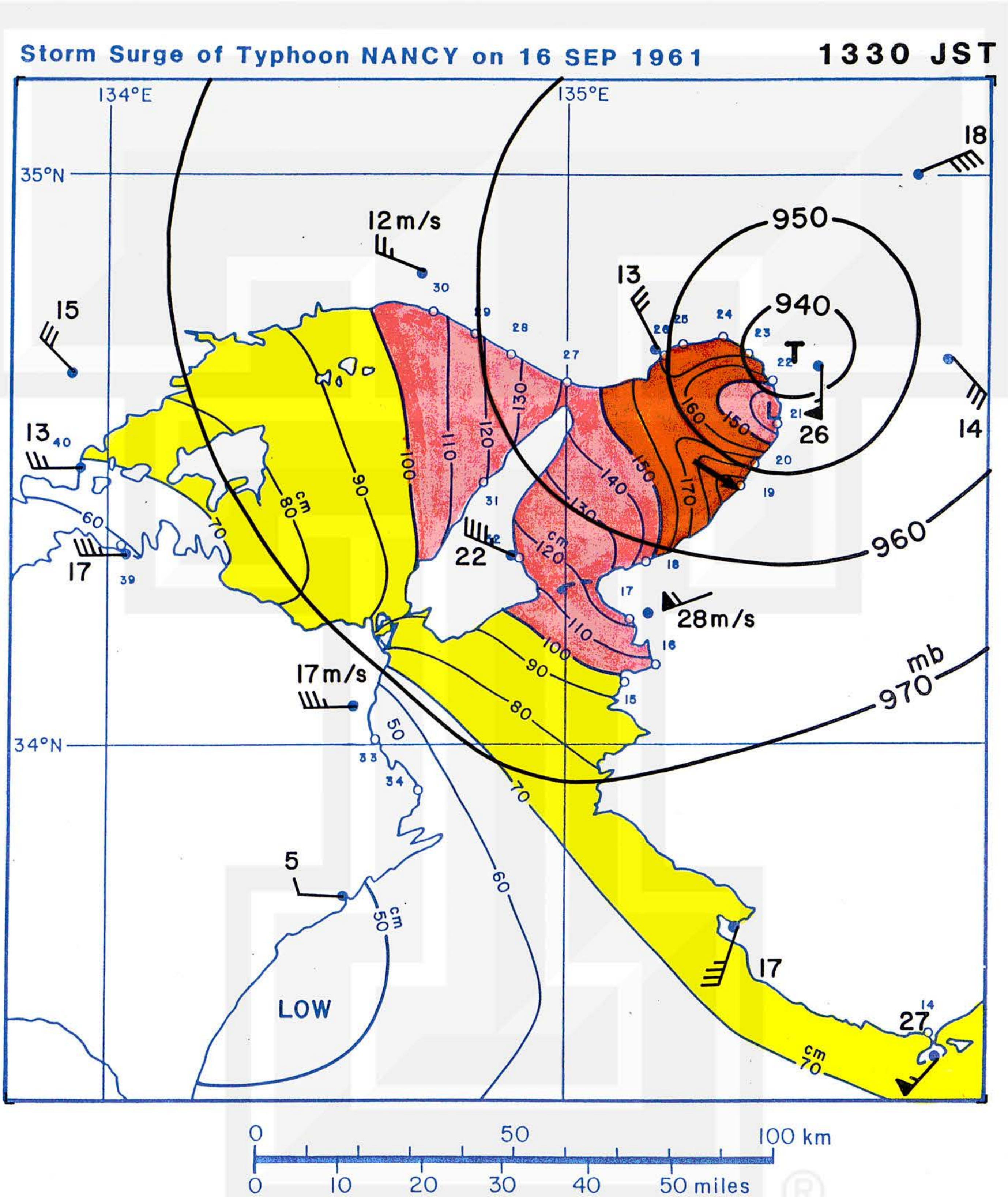

Fig. 5.7 Pattern of sea-level height anomalies at 1330 JST, 16 SEP 1961.

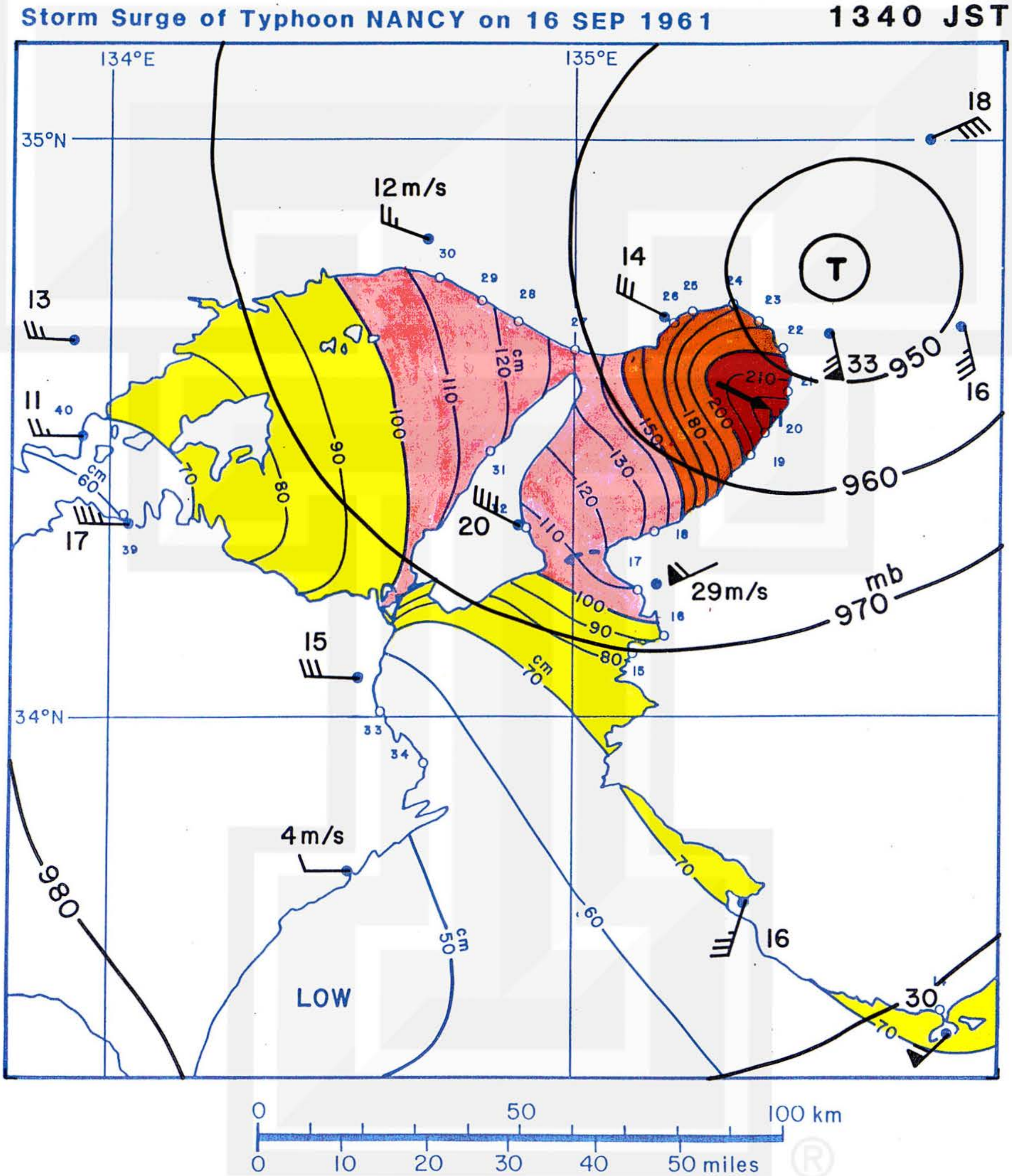

Fig. 5.8 Pattern of sea-level height anomalies at 1340 JST, 16 SEP 1961.

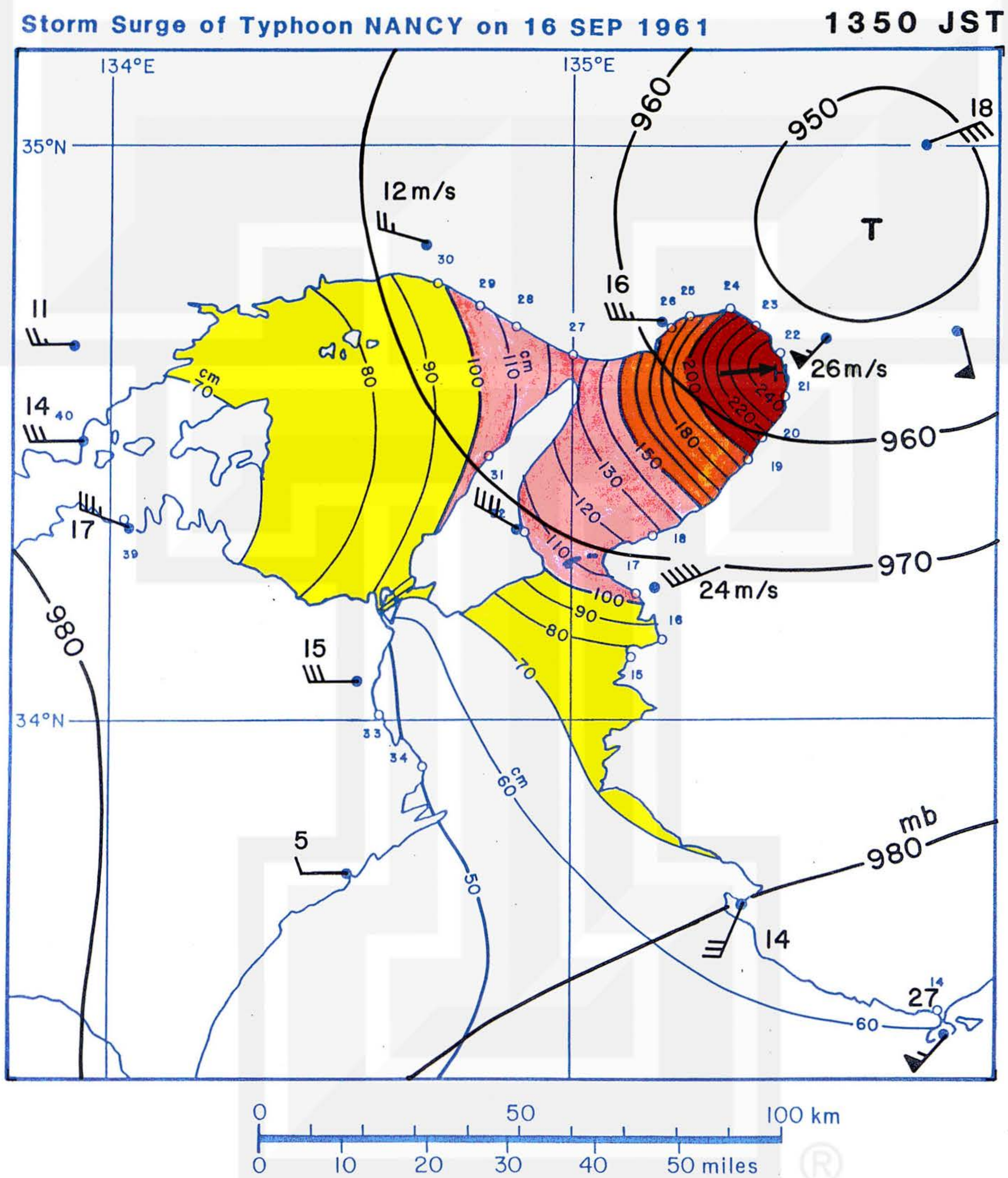

Fig. 5.9 Pattern of sea-level height anomalies at 1350 JST, 16 SEP 1961.

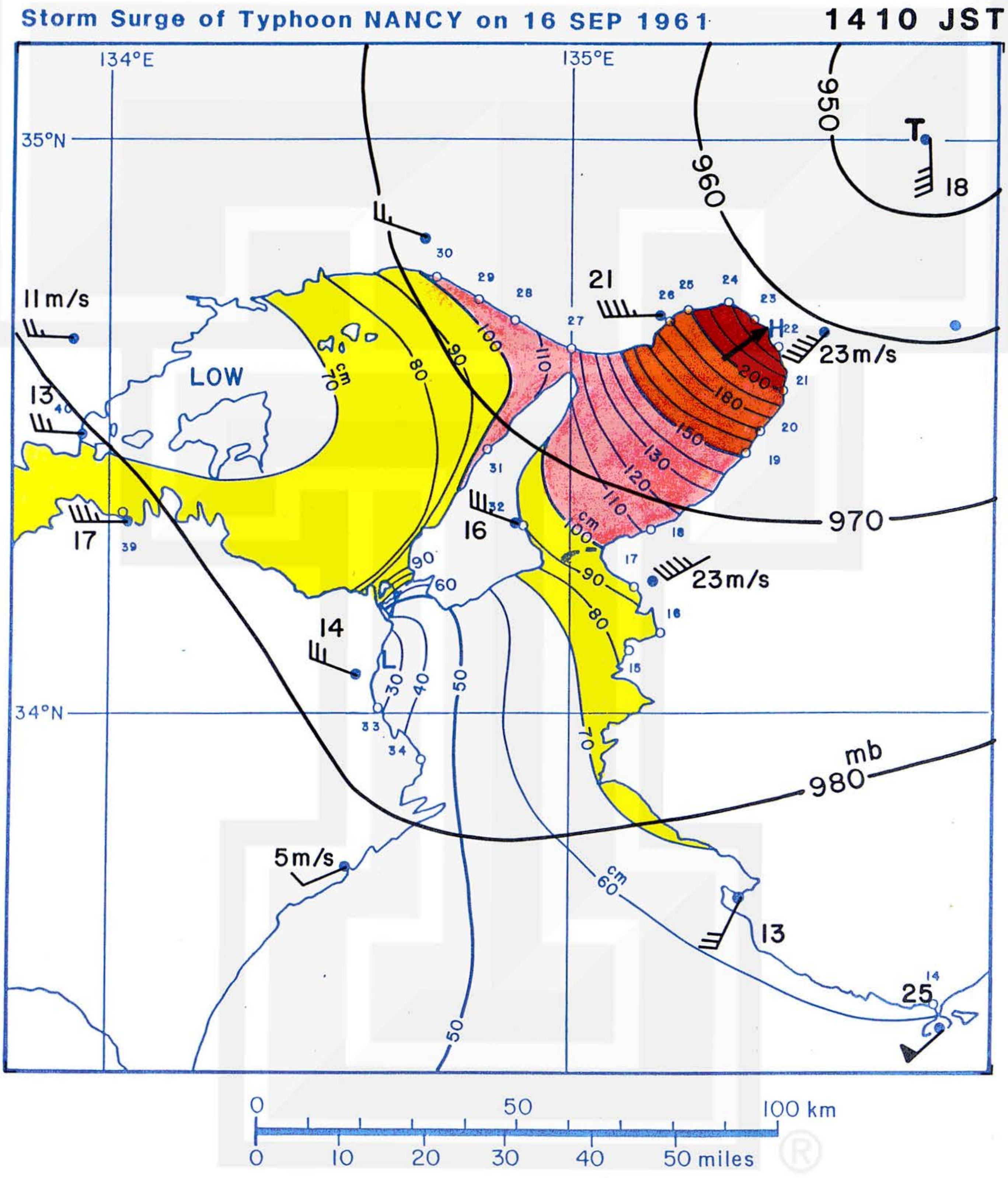

Fig. 5.10 Pattern of sea-level height anomalies at 1410 JST, 16 SEP 1961.

6. LOCAL PHOTOGRAPHS

In spite of efforts to obtain high quality action pictures of Typhoon Nancy, it was not possible to aquire good negatives and/or prints. All that could be obtained were positive transparencies that had to be converted into negatives, from which the pictures presented in this section were made.

Furthermore, I was not able to determine where the 16 pictures in Figures 6.1 through 6.4 were taken. It is extremely likely that the photographic sites are located along the coastline between Cape Muroto (see Fig. 2.1) and Cape Muroto Harbor. Any one of these pictures implies that the peak gust of the typhoon was as strong as 189+ mph, as was estimated at the Muroto Weather Station overlooking the Pacific Ocean.

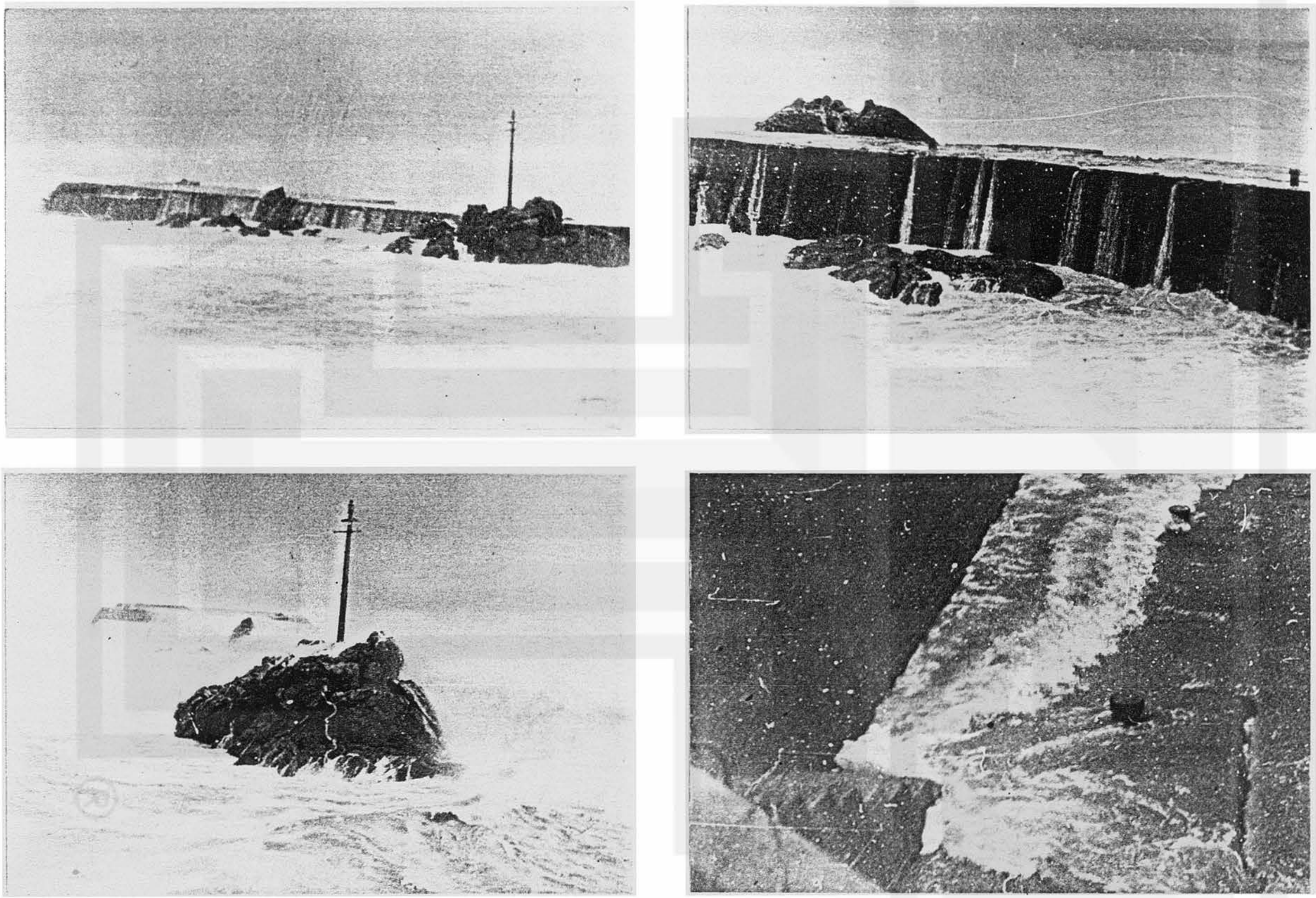

Fig. 6.1 Storm surge and wave action of Typhoon Nancy at seawall locations estimated to be in Cape Muroto Harbor and vicinity on the east side of Cape Muroto.

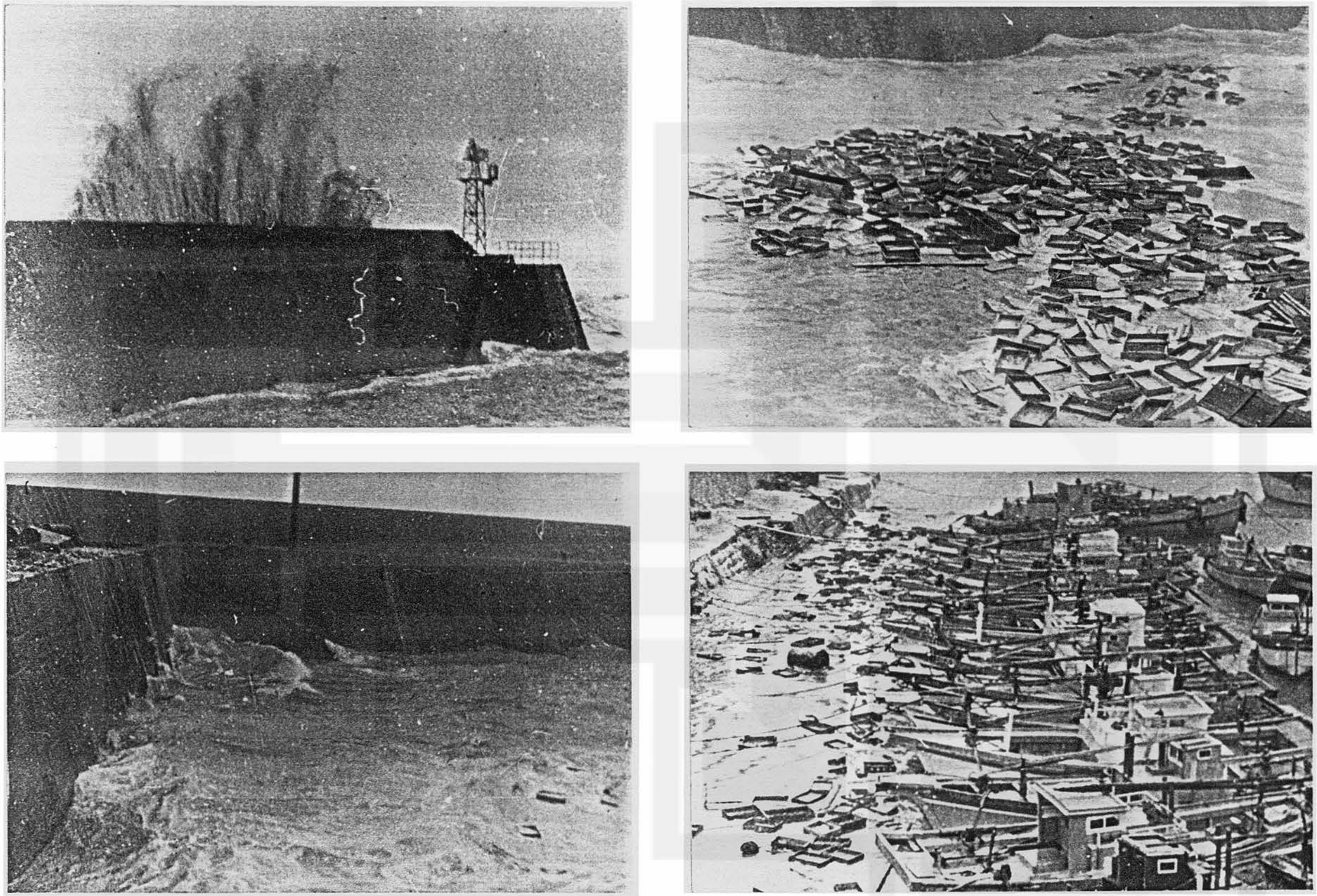

Fig. 6.2 Splash of typhoon waves crashing against the waterbreaks of the harbor (left). Drifting boxes and fishing boats fill the inside of the harbor (right).

Fig. 6.3 Coastal dikes and houses left destroyed or heavily damaged in the wake of Typhoon Nancy. An unidentified youngster observes the damage which most likely left a lasting impression.

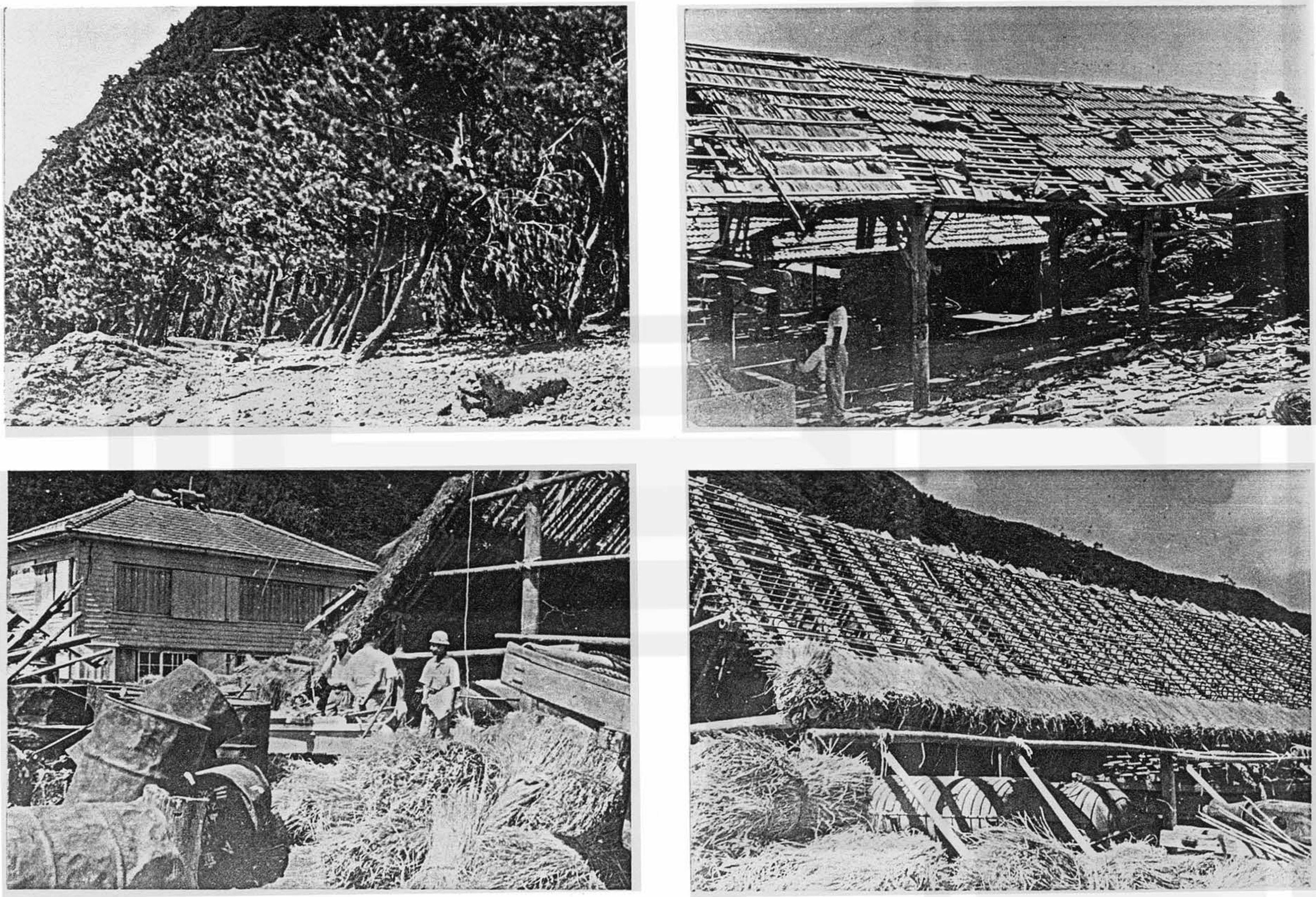

Fig. 6.4 Subtropical trees that were pushed over by Nancy's fury; and pole barns with straw roofs in the process of being repaired.